Advanced ERC Grant:
OSYRIS

Advanced ERC Grant:
QUAGATUA

EU IP SIQS

AvH
Feodor
Lynen

Generalitat de Catalunya

SGR 874

CERCA/Program

Obra Social
Fundación "la Caixa"

MPG
MPI
Garching

European Commission

EU FET-Proactive
QUIC

# Detection of topological order with quantum simulators

FNP
Polish Science Foundation

Symfonia

NCN
Narodowe Centrum Nauki

Fundació Privada CELLEX

EU STREP EQuaM

John Templeton Foundation

ICFO The Institute of Photonic Sciences

INTERNATIONAL YEAR OF LIGHT 2015

GOBIERNO DE ESPAÑA
MINISTERIO DE CIENCIA E INNOVACIÓN

FOQUS and
FISICATEAMO

EXCELENCIA SEVERO OCHOA

*iCrea
INSTITUCIÓ CATALANA DE RECERCA I ESTUDIS AVANÇATS

Fundació Catalunya - La Pedrera

# ICFO – Quantum Optics Theory
# Teoretyczna Optyka Kwantowa

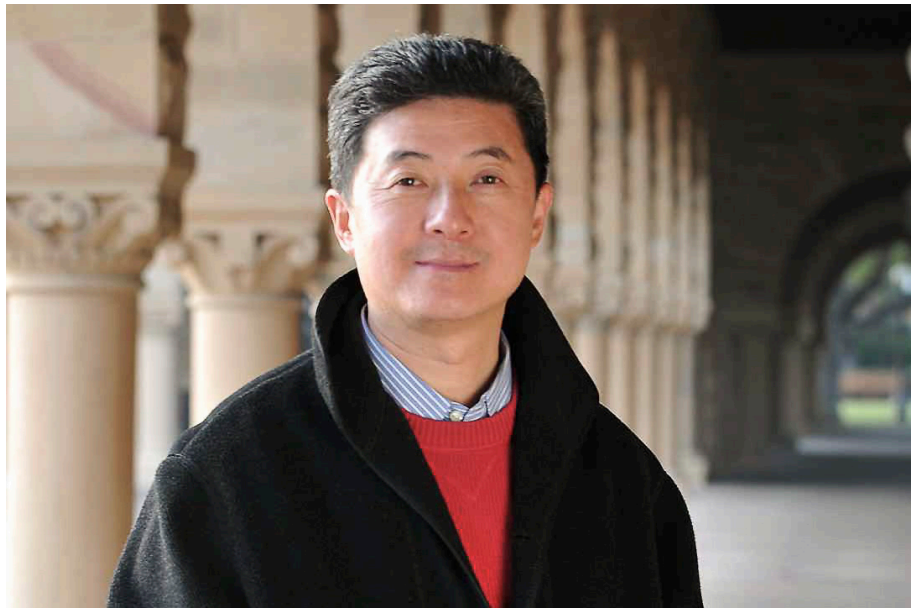

**RoY J. GLAUBer and shoucheng zhang**
**in memoriam**

# Detection of topological order with quantum simulators

0. Introduction
   - 0.1 Topology
   - 0.2 Quantum simulators
   - 0.3 Topology in quantum simulators
1. Detection of topological order in 1D chiral systems
   - 1.1 Chiral Mean Displacement
   - 1.2 Topological Anderson Insulator
   - 1.3 Photonic random walk in 1D
2. Detection of Chern number in 2D systems
   - 2.1 Measuring Chern numbers in Hofstadter strips
   - 2.2 Probing topology by "heating"
   - 2.3 Loading ultracold gases in Topological Floquet Bands
   - 2.4 Photonic random walk in 2D
3. Detection of topological order in 1D interacting systems
   - 3.1 Bosonic Peierls mechanism – minimal instance of lattice dynamics
   - 3.2 Phase diagram of $Z_2$ Bose-Hubbard model
   - 3.3 Correlated symmetry-protected topological states
   - 3.3 Self-adjusted pumping

ICFO
Institut de Ciències Fotòniques

# 0. Introduction

ICFO The Institute of Photonic Sciences

INTERNATIONAL YEAR OF LIGHT 2015

*iCrea

INSTITUCIÓ CATALANA DE RECERCA I ESTUDIS AVANÇATS

# Topology

Properties that remain unchanged under **continuous** and **smooth deformations**

**Genus:** number of holes of a closed surface

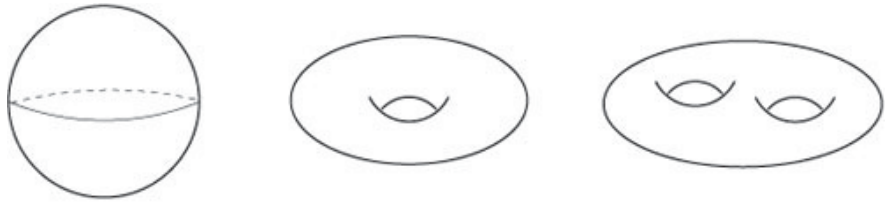

# Topological insulators

- Characterised by **global topological invariants**
- Classified on the basis of their **symmetries** and **dimensionality**
- **Topologically protected edge-states** in systems with boundaries
- **Bulk-edge correspondence**: the number of states on each edge is given by the invariant
- Beyond the periodic table: interacting/ **Anderson** / **Floquet TIs**, …

IQHE, Hofstadter, Chern insulators

chiral

| | | | | # of dimensions | | | | | | | |
|---|---|---|---|---|---|---|---|---|---|---|---|
| Class | $T$ | $C$ | $S$ | 0 | 1 | 2 | 3 | 4 | 5 | 6 | 7 |
| A | 0 | 0 | 0 | $\mathbb{Z}$ | 0 | $\mathbb{Z}$ | 0 | $\mathbb{Z}$ | 0 | $\mathbb{Z}$ | 0 |
| AIII | 0 | 0 | 1 | 0 | $\mathbb{Z}$ | 0 | $\mathbb{Z}$ | 0 | $\mathbb{Z}$ | 0 | $\mathbb{Z}$ |
| AI | + | 0 | 0 | $\mathbb{Z}$ | 0 | 0 | 0 | $2\mathbb{Z}$ | 0 | $\mathbb{Z}_2$ | $\mathbb{Z}_2$ |
| BDI | + | + | 1 | $\mathbb{Z}_2$ | $\mathbb{Z}$ | 0 | 0 | 0 | $2\mathbb{Z}$ | 0 | $\mathbb{Z}_2$ |
| D | 0 | + | 0 | $\mathbb{Z}_2$ | $\mathbb{Z}_2$ | $\mathbb{Z}$ | 0 | 0 | 0 | $2\mathbb{Z}$ | 0 |
| DIII | − | + | 1 | 0 | $\mathbb{Z}_2$ | $\mathbb{Z}_2$ | $\mathbb{Z}$ | 0 | 0 | 0 | $2\mathbb{Z}$ |
| AII | − | 0 | 0 | $2\mathbb{Z}$ | 0 | $\mathbb{Z}_2$ | $\mathbb{Z}_2$ | $\mathbb{Z}$ | 0 | 0 | 0 |
| CII | − | − | 1 | 0 | $2\mathbb{Z}$ | 0 | $\mathbb{Z}_2$ | $\mathbb{Z}_2$ | $\mathbb{Z}$ | 0 | 0 |
| C | 0 | − | 0 | 0 | 0 | $2\mathbb{Z}$ | 0 | $\mathbb{Z}_2$ | $\mathbb{Z}_2$ | $\mathbb{Z}$ | 0 |
| CI | + | − | 1 | 0 | 0 | 0 | $2\mathbb{Z}$ | 0 | $\mathbb{Z}_2$ | $\mathbb{Z}_2$ | $\mathbb{Z}$ |

Chern number

Winding

Chiu, Teo, Schnyder & Ryu, Rev. Mod. Phys. (2016)

# Topology in condensed matter systems

**Integer Quantum Hall effect – 1980**
2D semiconductor at very low temperature under a strong magnetic field

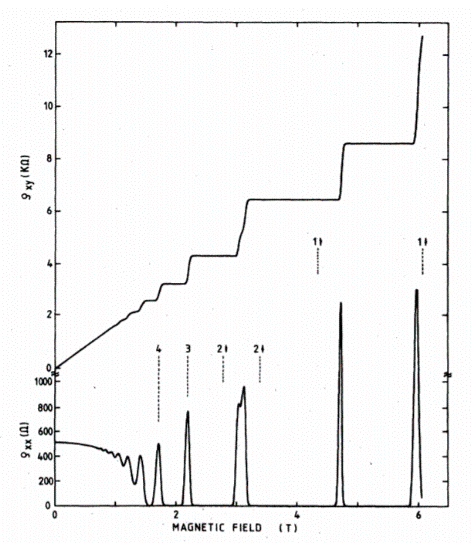


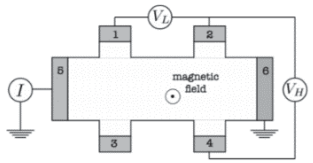


K. von Klitzing, *Nobel lecture*

**Quantum Spin Hall effect – 2007**
HgTe quantum well

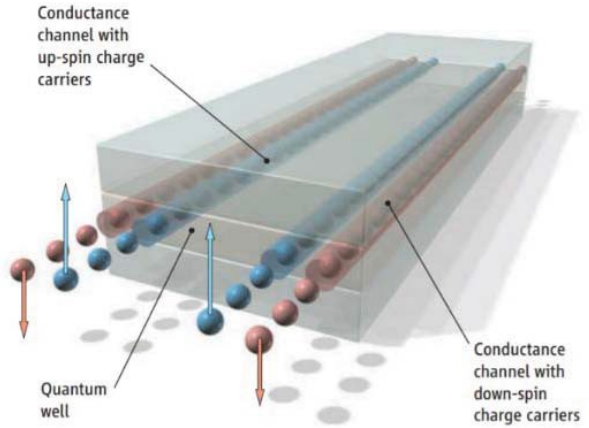


M. Konig et al., *Science* **318**: 766 (2007)

Enormous progresses in the last ten years

# Quantum simulators

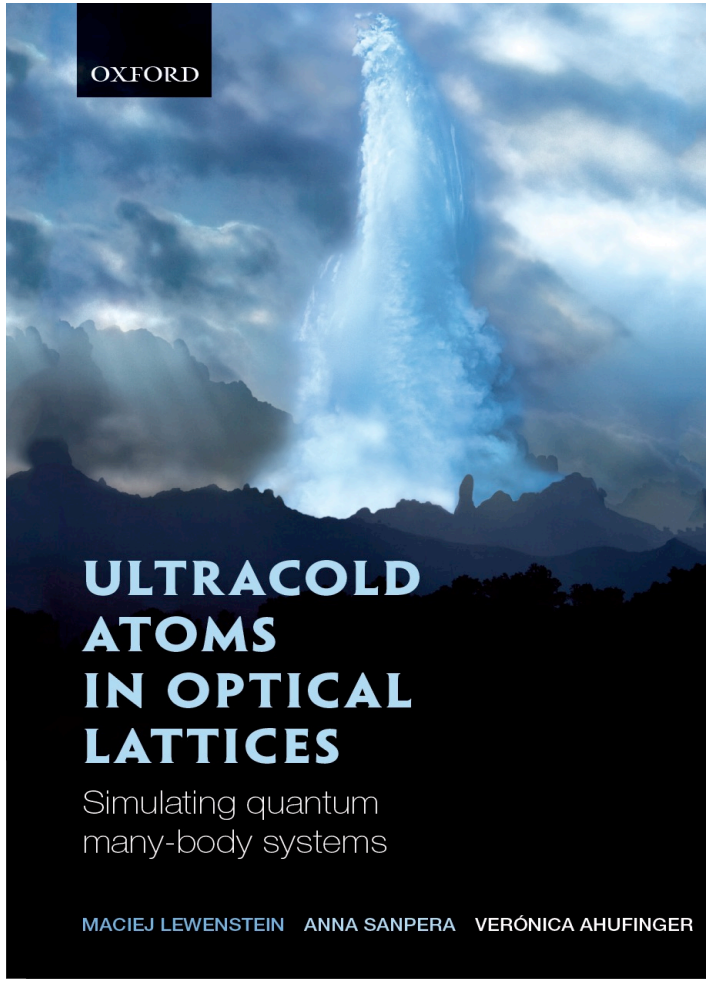


Ultracold atoms in optical lattices: Simulating quantum many-body physics
M. Lewenstein, A. Sanpera, V. Ahufinger, Oxford University Press (2012), reprint-paperback (2017)

# Simulators and quantum simulators

Controllable experimental platforms simulating the dynamics of the system of interest

**Water bath - 2017**
black holes

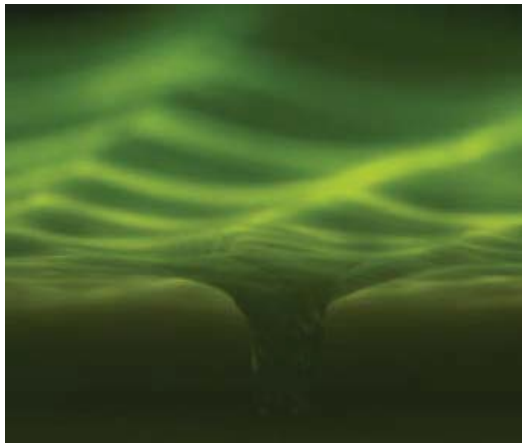

*T. Torres et al., Nat. Phys.* **13**:883

**Ultracold atoms in optical lattice - 2002**
Superfluid – Mott insulator transition

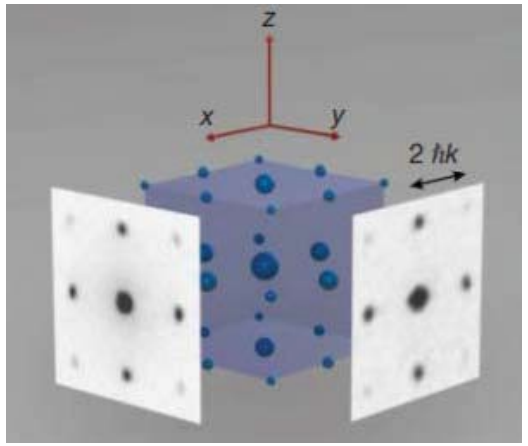


*M. Greiner et al., Nature* **415**:39–44

Many simulations of condensed matter systems with ultracold atoms and photons in the last 10 years

# Topology in quantum simulators

## With ultracold atoms:

### Laser assisted

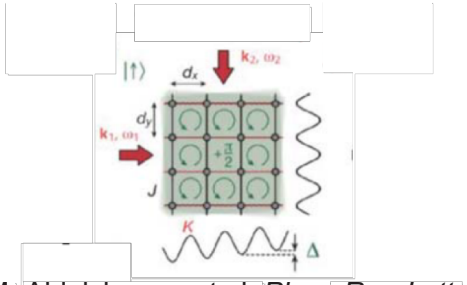

M. Aidelsburger et al., *Phys. Rev. Lett* (2013)

### Time-periodic lattice

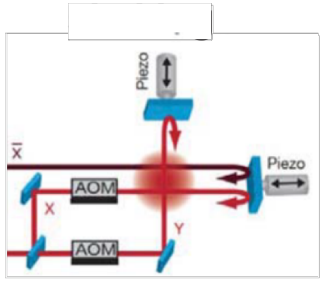


G Jotzu et al., *Nature* (2014)

### Synthetic dimension

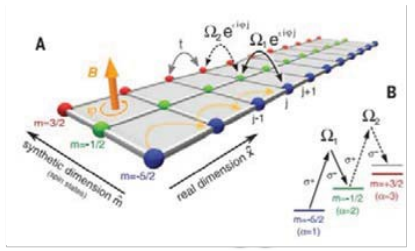

Mancini et al. *Science* (2015)
Stuhl et al. Science (2015)

## With photons:

### Array of shaped waveguides

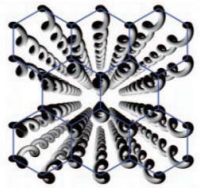

M.C.Rechtsman et al., *Nature* (2013)

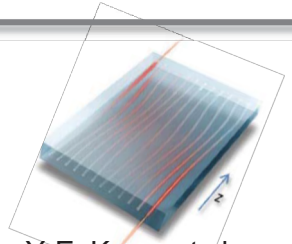

Y. E. Kraus et al., *Phys.Rev. Lett.* (2012)

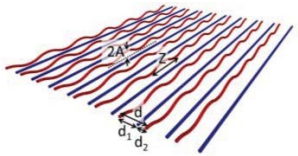

J. M. Zeuner et al., *Phys. Rev. Lett.* (2015)

### Quantum walk

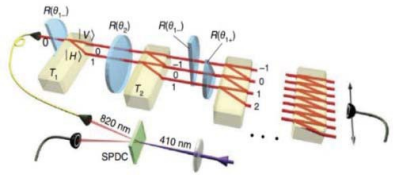


T. Kitagawa et al., *Nat. Commun.* (2012)

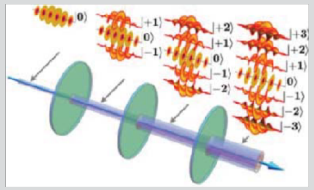

F. Cardano et al., *Sci. Adv.*, (2015)
F. Cardano,...**M.M.**...,
*Nat. Commun.* (2017)

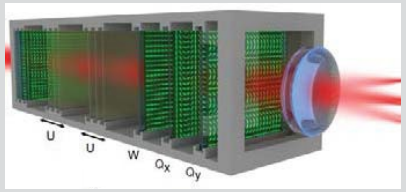

A.D'Errico...**M.M.**...., arXiv:(2018)

# Topology in quantum simulators

## With ultracold atoms:

**Laser assisted tunneling**

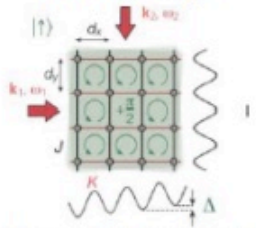

M. Aidelsburger et al.,*Phys. Rev. Lett.* (2013)

**Time-periodic lattice shaking**

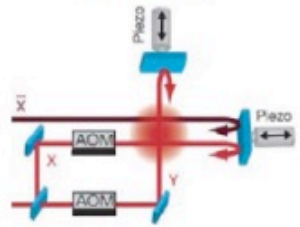


G. Jotzu et al., *Nature* (2014)

**Synthetic dimension**

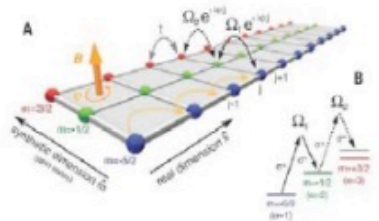

Mancini et al., *Science* (2015)

## With photons:

**Array of shaped waveguides**

M.C.Rechtsman et al., *Nature* (2013)

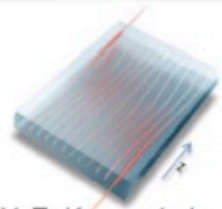

Y. E. Kraus et al., *Phys.Rev. Lett.* (2012)

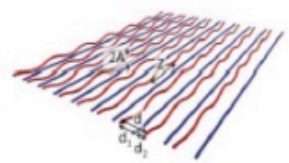

J. M. Zeuner et al., *Phys. Rev. Lett.* (2015)

**Quantum walk**

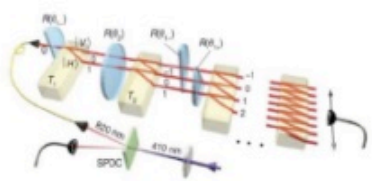

T. Kitagawa et al., *Nat. Commun.* (2012)

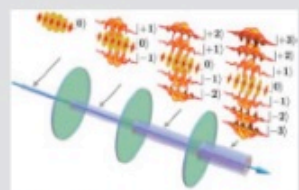

F. Cardano et al.,*Sci. Adv.*, (2015)
F. Cardano,...**M.M.**...,
*Nat. Commun.* (2017)

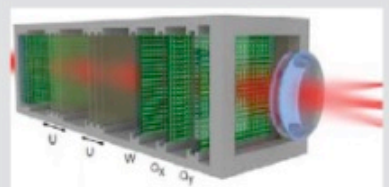

A.D'Errico...**M.M.**..., arXiv:(2018)

# Detecting topology in simulators

Edge states

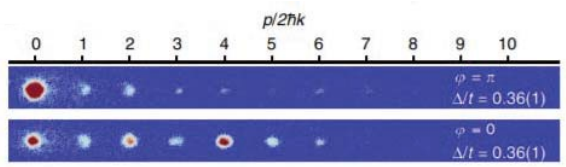


E.J. Meier et al., *Nat. Commun.* (2016)

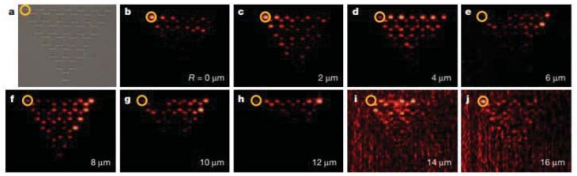

M.C.Rechtsman et al., *Nature* (2013)

Transverse displacement under external driving

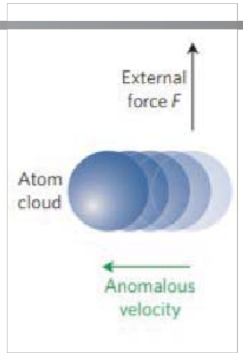


M. Aidelsburger et al., *Nat. Phys.* (2015)

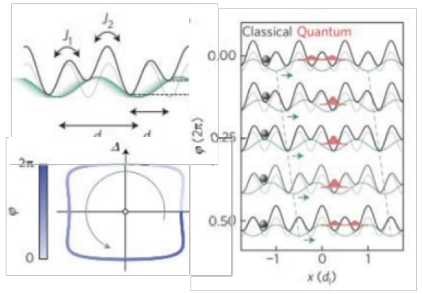


M. Lohse et al., *Nat. Phys.* (2015)

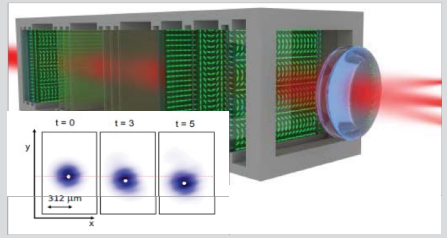

A.D'Errico...**M.M.**..., arXiv:1811.04001 (2018)

Direct measure of the topological invariant

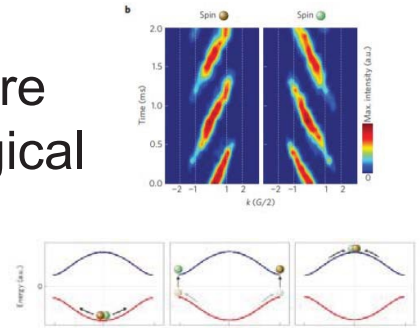

M. Atala et al., *Nat. Phys.* (2013)

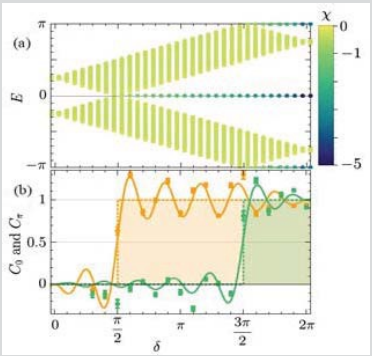

F. Cardano,...**M. M.**..., *Nat. Commun.* (2017)

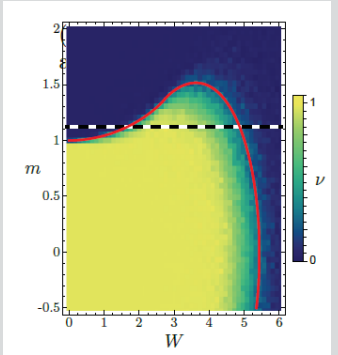

E. J. Meier...**M.M.**..., *Science* (2018)

# 1. Detection of topological order in 1D chiral systems

ICFO The Institute of Photonic Sciences

INTERNATIONAL YEAR OF LIGHT 2015

*iCrea

INSTITUCIÓ CATALANA DE RECERCA I ESTUDIS AVANÇATS

# Detecting topology in 1D chiral systems: the mean chiral displacement

- *Detection of Zak phases and topological invariants in a chiral quantum walk of twisted photons*,
  F. Cardano, A. D'Errico, A. Dauphin, **M.M.**, B. Piccirillo, C. de Lisio, G. De Filippis, V. Cataudella, E. Santamato, L. Marrucci, M. Lewenstein and P. Massignan, Nature Communications **8**:15516 (2017)

- *Topological characterization of chiral models through their long time dynamics*,
  **M.M.,** A. Dauphin, F. Cardano, M. Lewenstein and P. Massignan, New Journal of Physics **20** (2018)

- *Observation of the topological Anderson Insulator in disordered atomic wires*,
  E. J. Meier, F. Alex An, A. Dauphin, **M.M.**, P. Massignan, T. L. Hughes, B. Gadway Science **362**:6417 (2018)

**Maria Maffei**: 1 PhD Thesis co-tutelle Università degli studi di Napoli Federico II and IFCO

# Chiral-symmetric topological insulators

The SSH model

$$H = \sum_n \left[ a c_n^\dagger \sigma_x c_n + b \left( c_{n+1}^\dagger \frac{(\sigma_x - i\sigma_y)}{2} c_n + \text{h.c.} \right) \right]$$

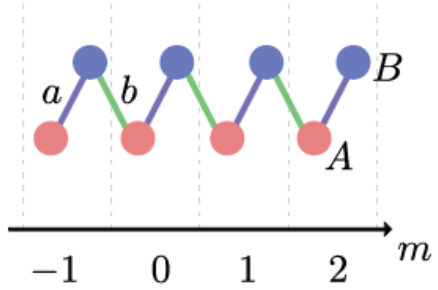


An Hamiltonian is **chiral-symmetric** if there exists an **Hermitian** and **unitary operator** such that:

$$\Gamma H \Gamma^{-1} \equiv \Gamma H \Gamma = -H \quad \text{with} \quad \Gamma^2 = 1$$

# Winding number

The winding number is the topological invariant characterising the Chiral class in 1D

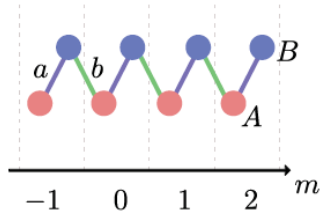


$$W = \int_{-\pi}^{\pi} \frac{dk}{2\pi i} Tr[h^{-1}\partial_k h]$$

$$H(k) = \begin{pmatrix} 0 & h(k)^\dagger \\ h(k) & 0 \end{pmatrix}$$

with $h(k) = a + be^{ik}$

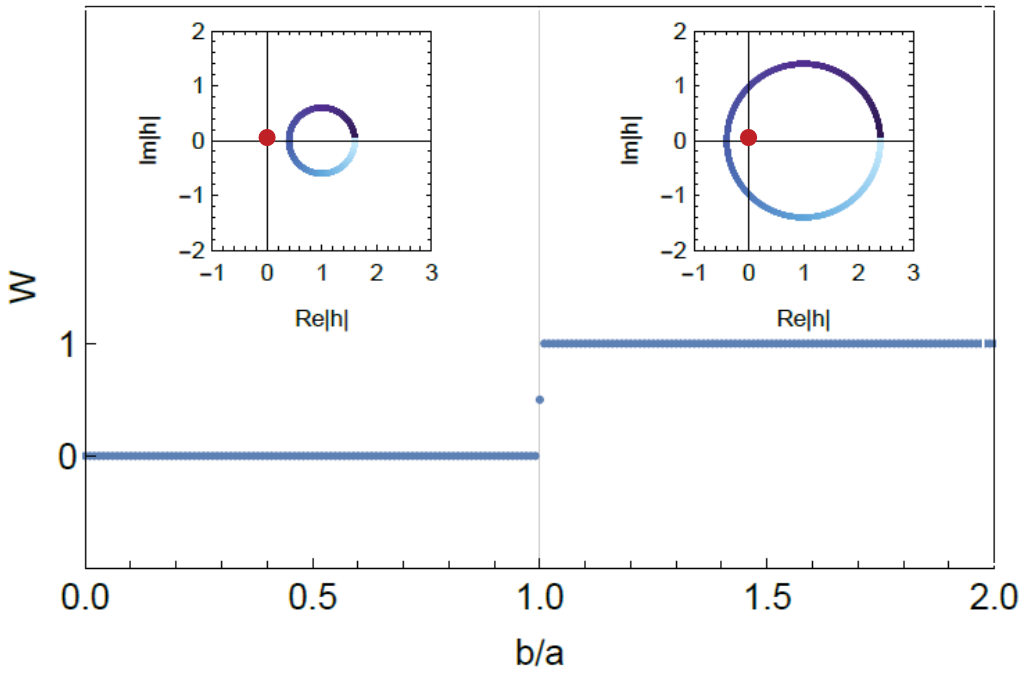

# Bulk-edge correspondence

In the limit of zero intra-cell hopping localised states arise at the edges of the chain

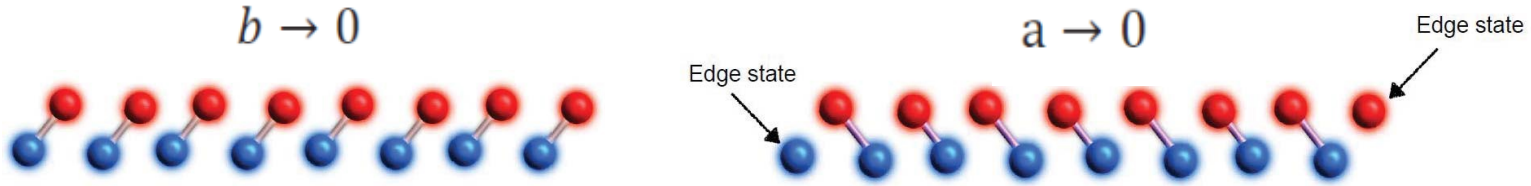


Bulk-edge correspondence: the winding number counts the states on each edge

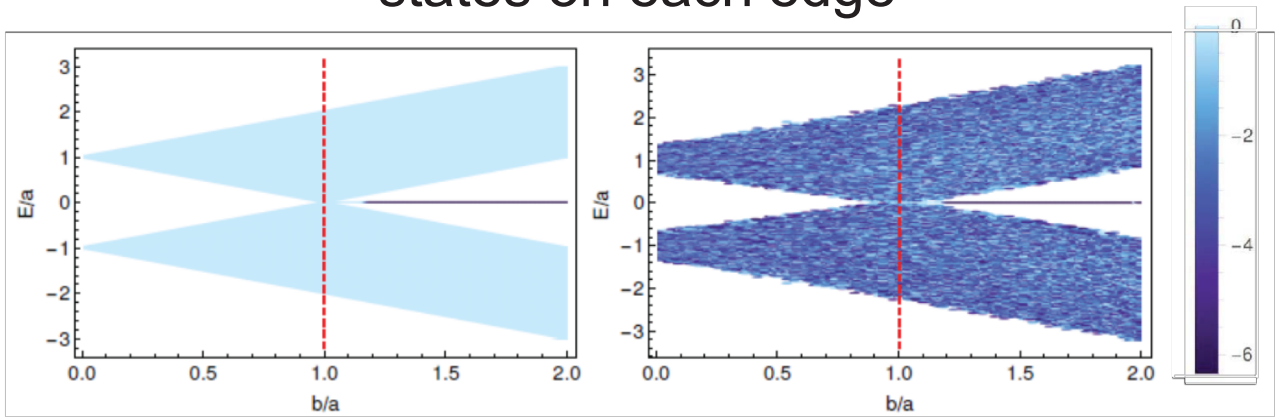


The edge states are topologically protected against chiral- and gap-preserving perturbations

# Winding number and Mean Chiral Displacement (MCD)

Starting from an arbitrary localized state

$$\overline{|\psi\rangle} = |\psi, 0\rangle$$

The MCD reads

$$C(t) \equiv 2\langle \Gamma m(t) \rangle_{\overline{|\psi\rangle}} = W + \dots$$

No external elements nor filled bands required for the MCD detection

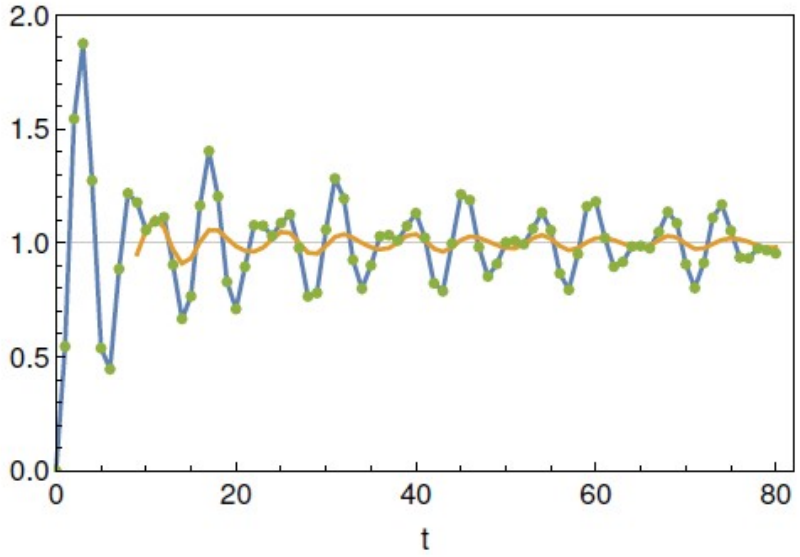


F. Cardano, A. D'Errico, A. Dauphin, **M.M.**, B. Piccirillo, C. de Lisio, G. De Filippis, V. Cataudella, E. Santamato, L. Marrucci, M. Lewenstein and P. Massignan, *Nat. Commun*. **8**:15516 (2017)

# Generalization of the method

The MCD detects the winding number in chiral systems with any internal dimension *D*

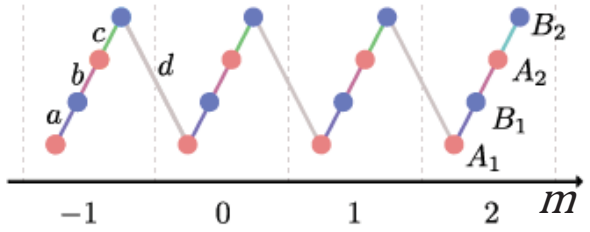


We write the MCD as the trace over a basis of the internal space

$$C(t) = \sum_{j=1}^{D} \langle \Gamma m(t) \rangle_{\overline{|\psi_j\rangle}} = W + \ \ldots$$

**M. M.** et al., *New J. Phys.* **20** (2018)

# Generalization of the method

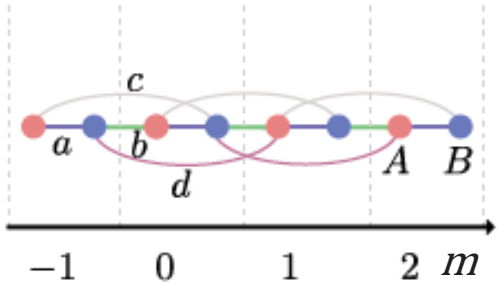


The MCD detects the Winding number in chiral systems with long-range hopping

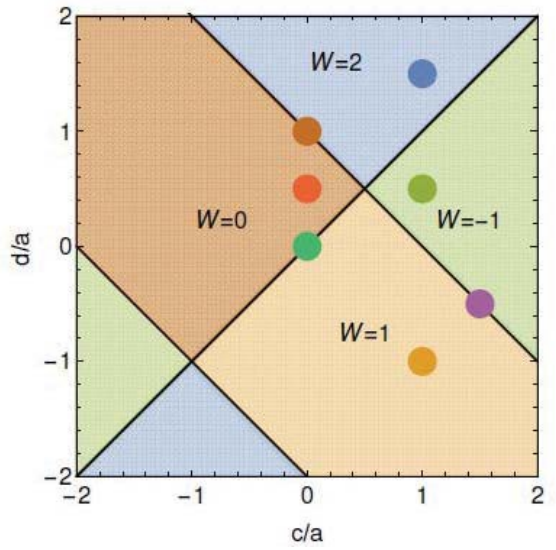


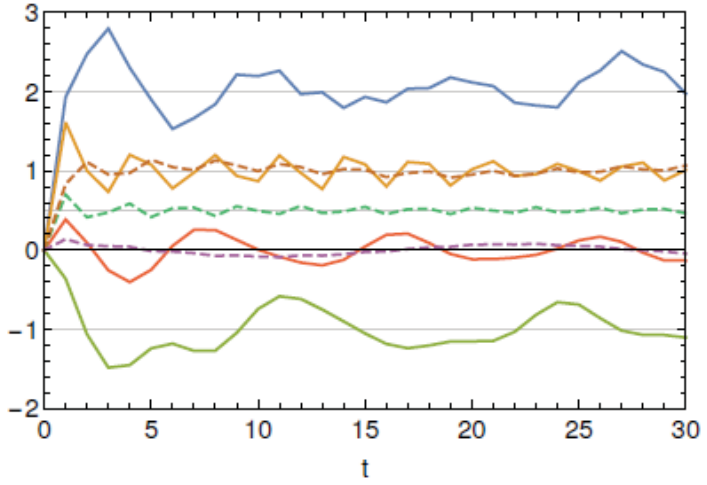


The MCD detects the Winding also at the transition points

**M. M.** et al., *New J. Phys.* **20** (2018)

# Topological Anderson Insulator (TAI)

In 1- and 2D a disorder can induce **Anderson localization**

A strong disorder can drive a system from a trivial to a topological phase

Theory

- In a 2D metallic quantum well
  J. Li et al., *Phys. Rev. Lett.*, **102**:136806 (2009)
- In a 1D chiral symmetric system
  A. Altland et al., *Phys. Rev.B,* **91**: 085429 (2015)
  I. Mondragon-Shem et al., *Phys. Rev. Lett.,* **113**: 046802 (2014)

Observation

- In a 2D array of optical waveguides

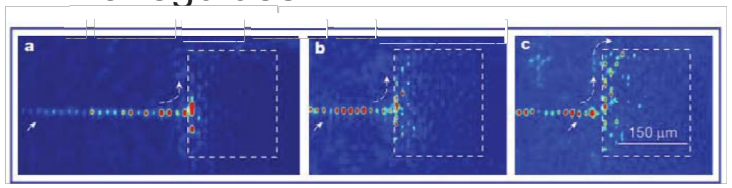

# Simulating the TAI with cold atoms

- Bose-Einstein condensate (BEC)
- Interference between a single and a multi-frequency beam
- Lattice of discrete momentum states of the BEC
- Laser-driven coupling between momentum states
- 1D Hamiltonian with tunable hopping

$$H_{\text{eff}} \approx \sum_j t_j (e^{i\varphi_j} |\tilde{\psi}_{j+1}\rangle\langle\tilde{\psi}_j| + \text{h.c.})$$

Phase difference between the laser fields

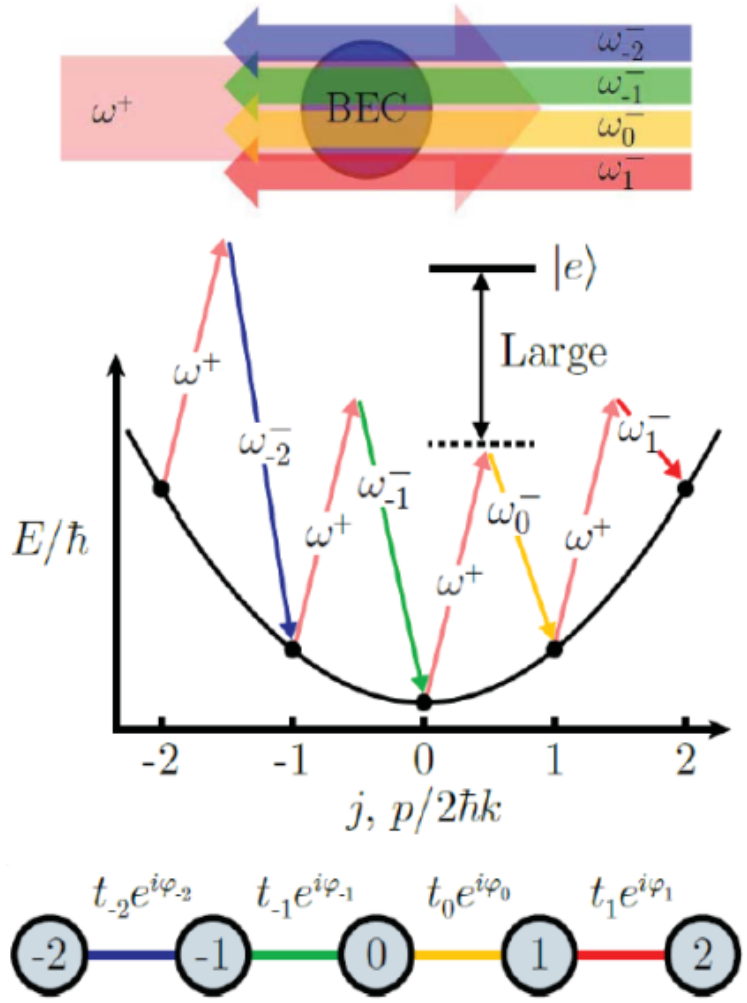


E. J. Meier, F. A. An, A. Dauphin, **M. M.**, P. Massignan, T. L. Hughes, B. Gadaway, *Science* **362**: 6417 (2018)

# Simulating the TAI with cold atoms

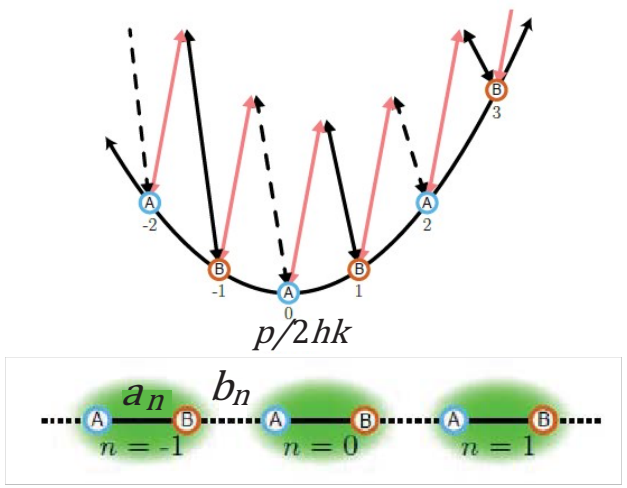


Random disorder can be included in the hopping

$$b_n = t$$
$$a_n = t(r + \Delta\,\omega_n) \qquad \text{with } \omega_n \,\epsilon[-0.5, 0.5]$$

Color map: real space Winding number for a system of 200 cells and 1000 disorder realizations

Red line: critical boundary (diverging localization length in the therm. limit)

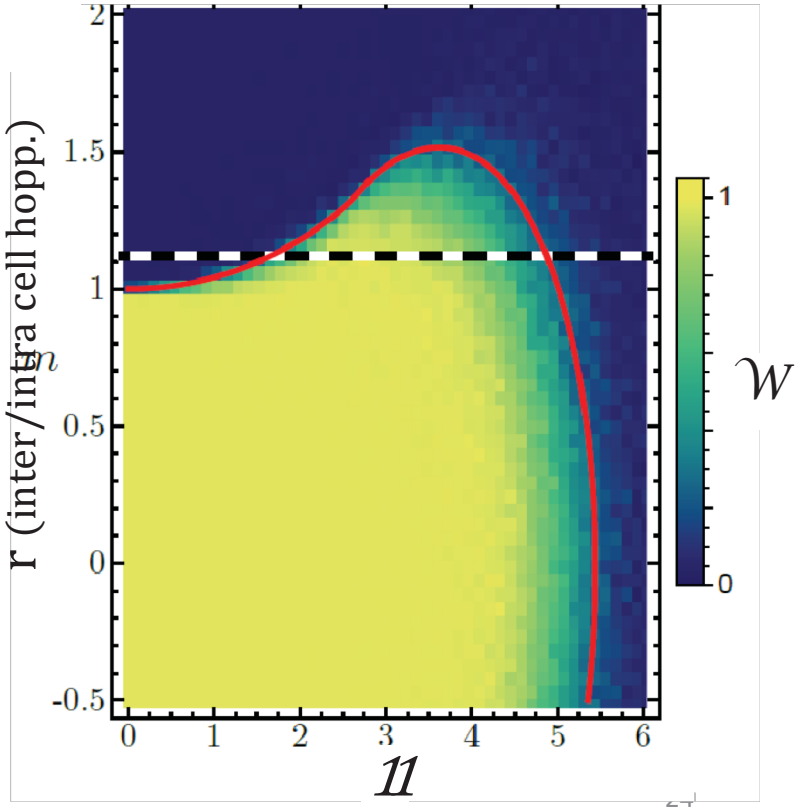


E. J. Meier, F. A. An, A. Dauphin, **M. M.**, P. Massignan, T. L. Hughes, B. Gadaway, *Science* **362**: 6417 (2018)

# Revealing the TAI phase through the MCD

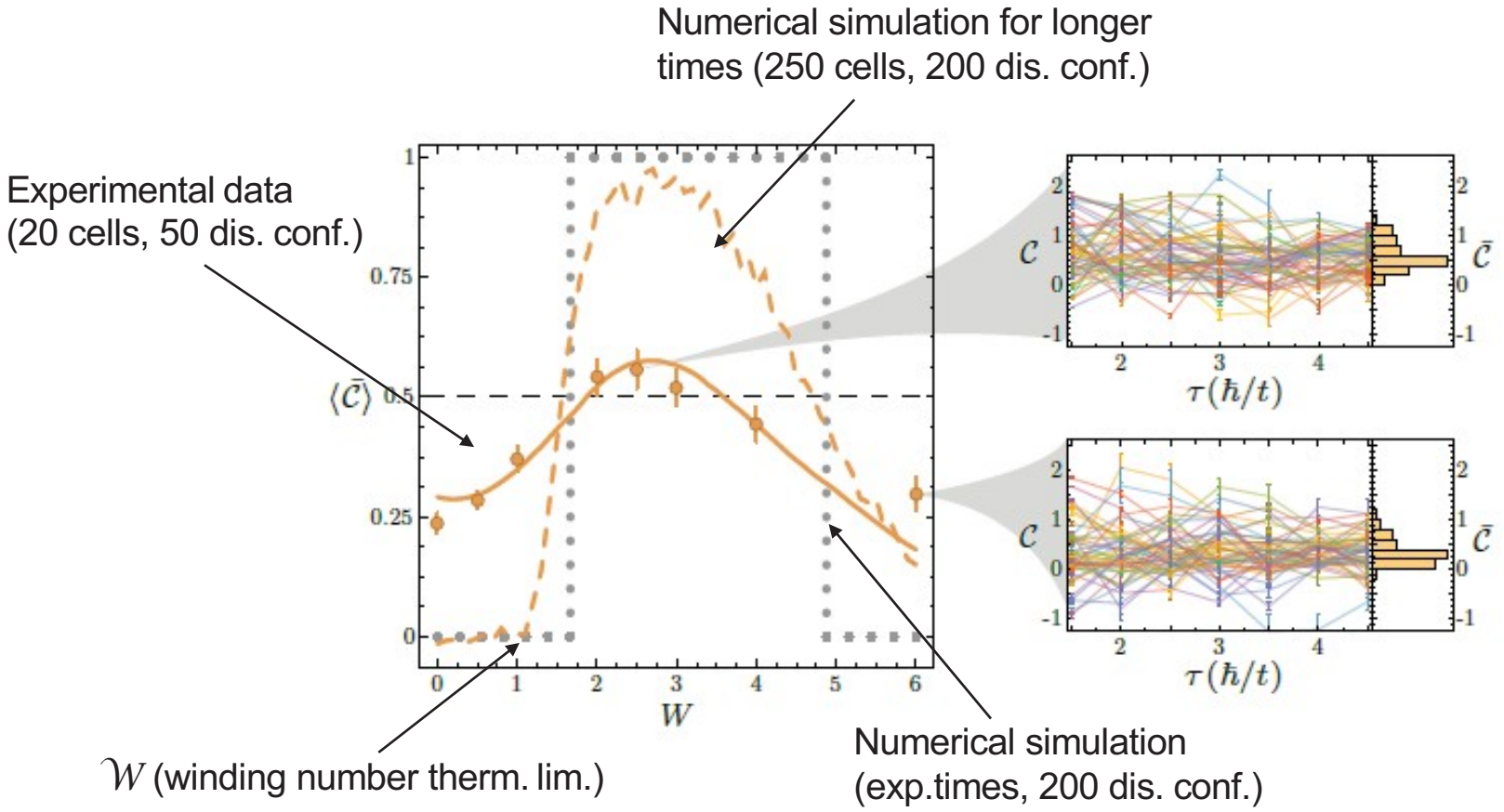


E. J. Meier, F.A. An, A. Dauphin, **M. M.**, P. Massignan, T. L. Hughes, B. Gadaway, *Science* **362**: 6417 (2018)

# Simulating a chiral insulator with a photonic 1D quantum walk

- Statistical moments of quantum-walk dynamics reveal topological quantum transitions, F. Cardano, **M.M.**, F. Massa, B. Piccirillo, C. de Lisio, G. De Filippis, V. Cataudella, E. Santamato and L. Marrucci, Nature Communications **7**:11439 (2016).

- Detection of Zak phases and topological invariants in a chiral quantum walk *of twisted photons*, F. Cardano, A. D'Errico, A. Dauphin, **M.M.**, B. Piccirillo, C. de Lisio, G. De Filippis, V. Cataudella, E. Santamato, L. Marrucci, M. Lewenstein and P. Massignan, Nature Communications **8**:15516 (2017).

# Quantum Walk (QW)

- **Periodic** repetition of unitary operations
- A **walker** with an internal degree of freedom (**coin**)
- At each step the coin state is rotated (W) and the walker is displaced (Q) on a lattice
- The direction of the walker displacement depends on the state of the coin
- The QW probability distribution arises from the quantum interference of the possible walker position states


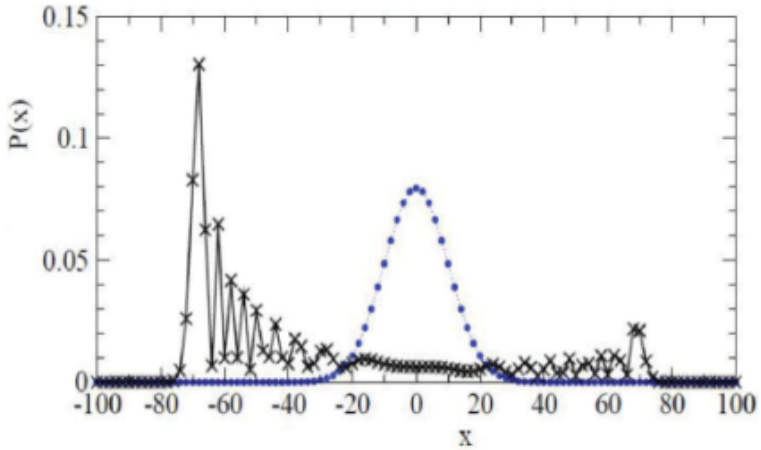


V. Kendon. Decoerence in quantum walk, a review (2007)

# Quantum Walk's effective Hamiltonian

**Time periodicity**
- Floquet theorem
- Effective Hamiltonian

**Spatial periodicity**
- Bloch theorem
- Effective Bloch Hamiltonian

$$U = Q \cdot W \qquad i \log U(k) = H_{eff}(k) = \mathrm{E}(k)\mathbf{n}(k) \cdot \boldsymbol{\sigma}$$

$$E = E + 2\pi n$$

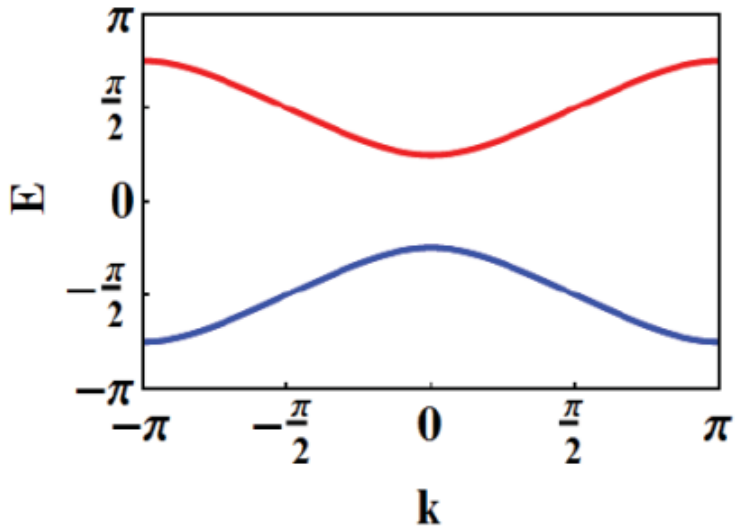

# Quantum Walk with light's Orbital Angular Momentum

- The walker position is the Orbital Angular Momentum of a light beam
- The coin is its polarization

$$|m\rangle \otimes |s\rangle = A(r)e^{ikz}\, e^{im\varphi} \otimes \left(\alpha|R\rangle + \beta|L\rangle\right)$$

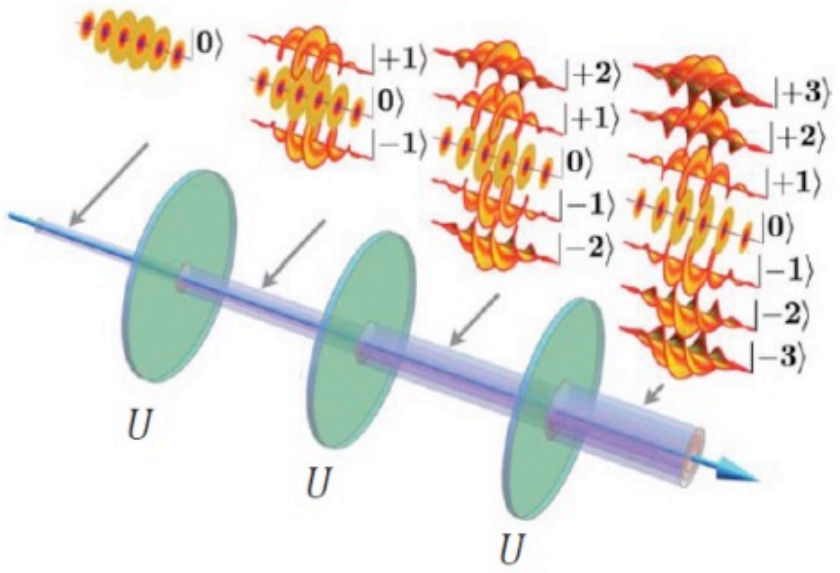


F. Cardano et al., *Sci. Adv.*, **1** (2015)

# Quantum Walk with light's Orbital Angular Momentum

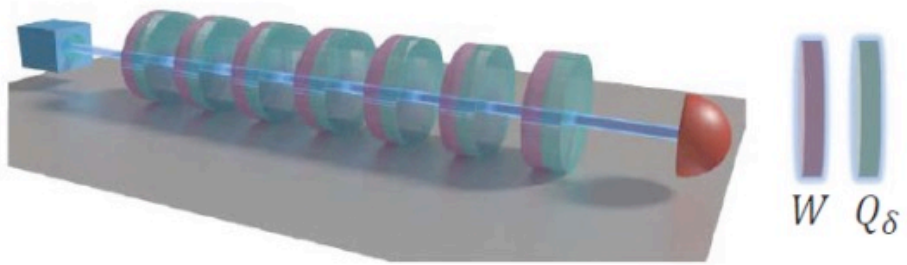


$$U_\delta = Q_\delta \cdot W$$

$$W = \begin{pmatrix} 1/\sqrt{2} & -i/\sqrt{2} \\ -i/\sqrt{2} & 1/\sqrt{2} \end{pmatrix}$$

Quarter-wave plate:
Polarization rotation

$$Q_\delta = \begin{pmatrix} \cos\left(\frac{\delta}{2}\right) & isin\left(\frac{\delta}{2}\right)e^{-ik} \\ isin\left(\frac{\delta}{2}\right)e^{ik} & \cos\left(\frac{\delta}{2}\right) \end{pmatrix}$$

Q-plate:
Polarization-dependent shift of the OAM with tunable efficiency

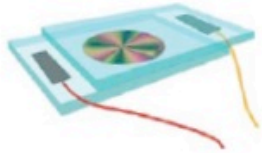

# Quantum Walk with light's Orbital Angular Momentum

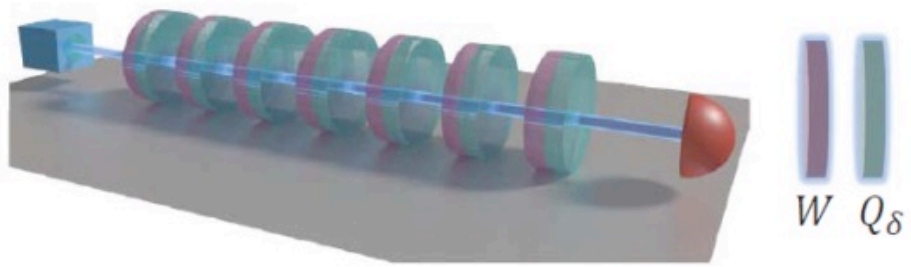


$$U_\delta = Q_\delta \cdot W$$

$$i \log U(k) = H_{eff}(k) = \mathrm{E}(k)\mathbf{n}(k) \cdot \boldsymbol{\sigma}$$

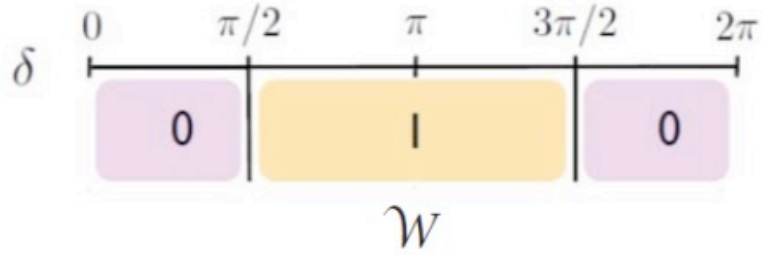


Topological quantum walk protocol

F. Cardano, **M.M.**, …, L. Marrucci, Nat. Commun. **7**:11439 (2016)

# Topological characterization of 1D chiral Quantum Walks

The Winding number is not enough to fully characterize the QW

We need **two invariants** to count the edge modes with energy 0 and π

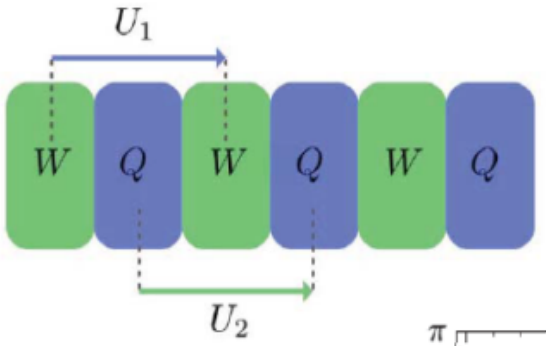


$$\{\mathcal{W}_0\,,\,\mathcal{W}_\pi\}=\{(\mathcal{W}_1+\mathcal{W}_2)/2\,,(\mathcal{W}_1-\mathcal{W}_2)/2\}$$

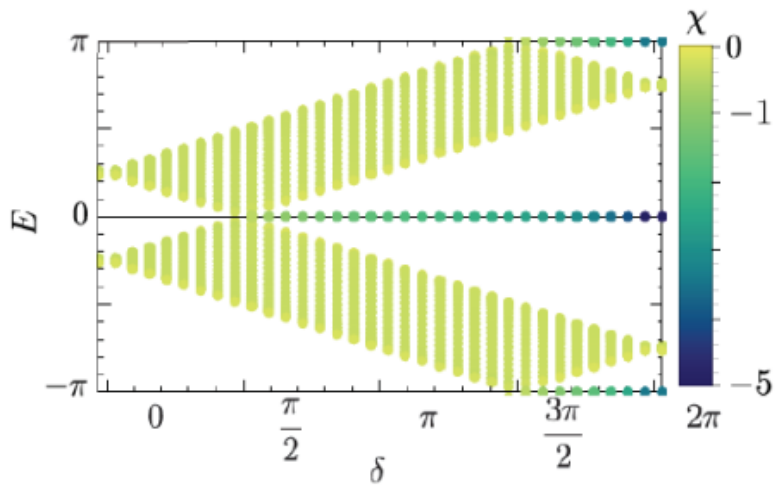


J.K. Asboth and H. Obuse, Phys. Rev. B **88**, 121406(R) (2013)

# Detection of the invariants through the MCD

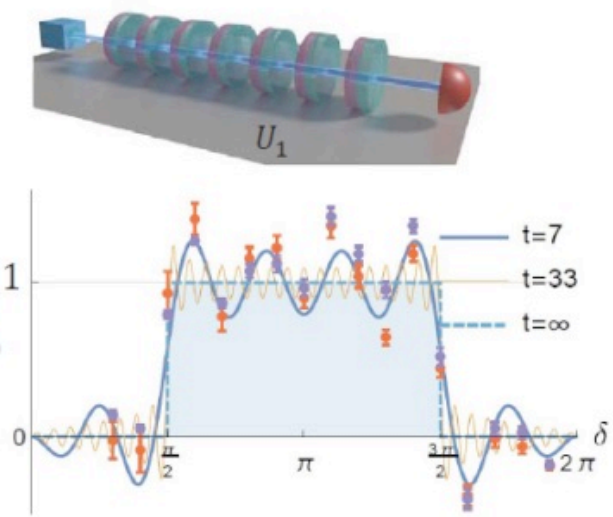


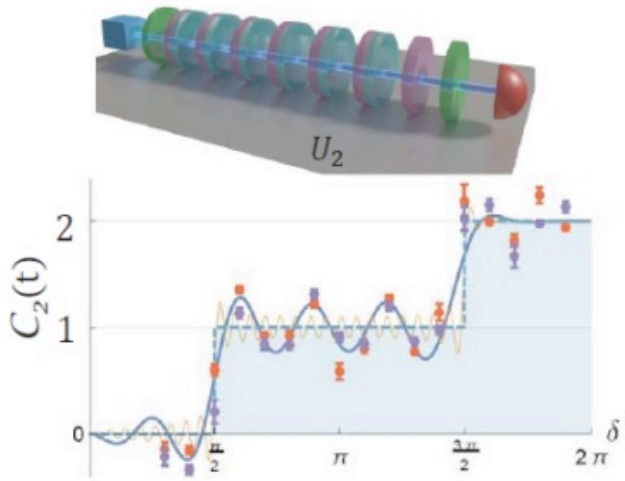


$$\{C_0, C_\pi\} = \{(C_1 + C_2)/2, (C_1 - C_2)/2\}$$

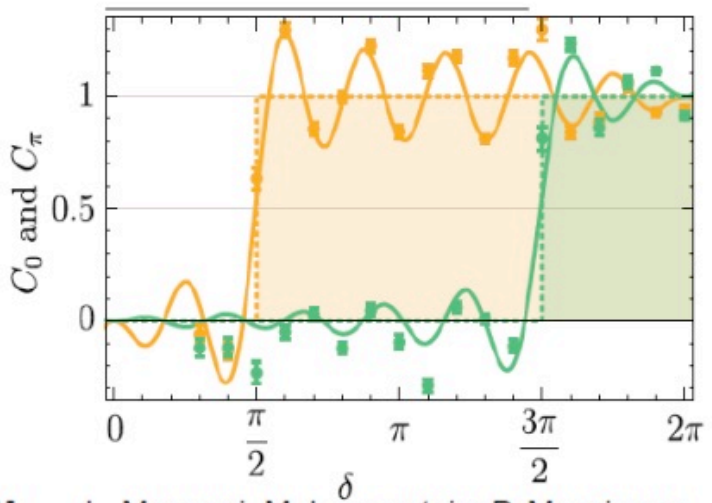


F. Cardano, A. D'Errico, A. Dauphin, **M. M.**,…, L. Marrucci, M. Lewenstein, P. Massignan, Nat. Commun. **8**: 15516 (2017)

# 2. Detection of Chern number in 2D systems

ICFO
The Institute of Photonic Sciences

INTERNATIONAL YEAR OF LIGHT 2015

*iCrea
INSTITUCIÓ CATALANA DE RECERCA I ESTUDIS AVANÇATS

**Sam Mugel**: 1 PhD Thesis co-tutelle University of Southhampton and ICFO

SciPost Phys. 3, 012 (2017)

# Measuring Chern numbers in Hofstadter strips

Samuel Mugel[1,2], Alexandre Dauphin[1], Pietro Massignan[1,3], Leticia Tarruell[1], Maciej Lewenstein[1,4], Carlos Lobo[2] and Alessio Celi[1⋆],

1 ICFO-Institut de Ciencies Fotoniques, The Barcelona Institute of Science and Technology, 08860 Castelldefels (Barcelona), Spain
2 Mathematical Sciences, University of Southampton, Highfield, Southampton, SO17 1BJ, United Kingdom
3 Departament de Física, Universitat Politècnica de Catalunya, Campus Nord B4-B5, E-08034 Barcelona, Spain
4 ICREA, Passeig de Lluís Companys, 23, E-08010 Barcelona, Spain

⋆ alessio.celi@icfo.eu

## Abstract

Topologically non-trivial Hamiltonians with periodic boundary conditions are characterized by strictly quantized invariants. Open questions and fundamental challenges concern their existence, and the possibility of measuring them in systems with open boundary conditions and limited spatial extension. Here, we consider transport in Hofstadter strips, that is, two-dimensional lattices pierced by a uniform magnetic flux which extend over few sites in one of the spatial dimensions. As we show, an atomic wave packet exhibits a transverse displacement under the action of a weak constant force. After one Bloch oscillation, this displacement approaches the quantized Chern number of the periodic system in the limit of vanishing tunneling along the transverse direction. We further demonstrate that this scheme is able to map out the Chern number of ground and excited bands, and we investigate the robustness of the method in presence of both disorder and harmonic trapping. Our results prove that topological invariants can be measured in Hofstadter strips with open boundary conditions and as few as three sites along one direction.

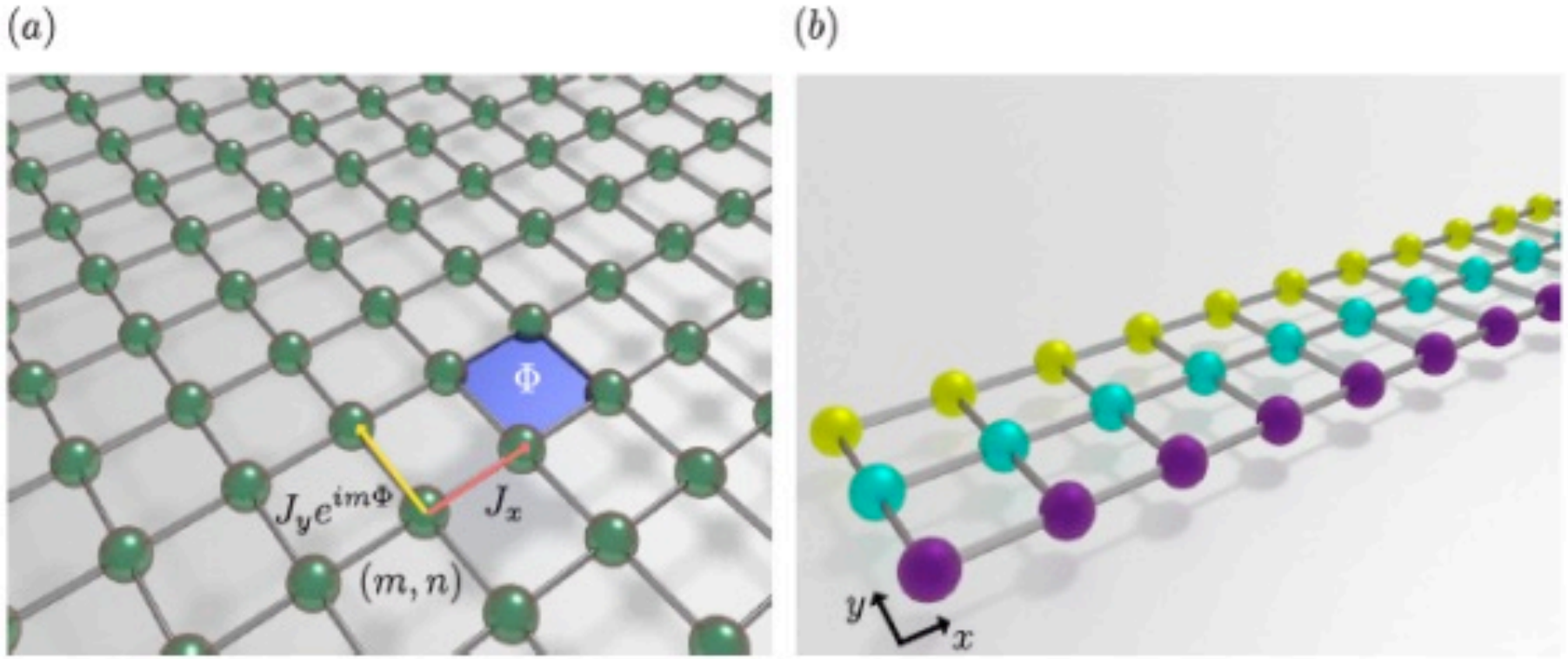


Figure 1: Sketch of the tunnelings of the Hofstadter Hamiltonian, Eq. (1). The site indices in the $x, y$ directions are $m, n$ respectively. The total flux through each plaquette is $\Phi = 2\pi p/q$. Panel (a) depicts the usual 2D Hofstadter extended lattice, while panel (b) shows an Hofstadter strip, which contains few states along the $y$ direction (in the example shown, $N_y = 3$).

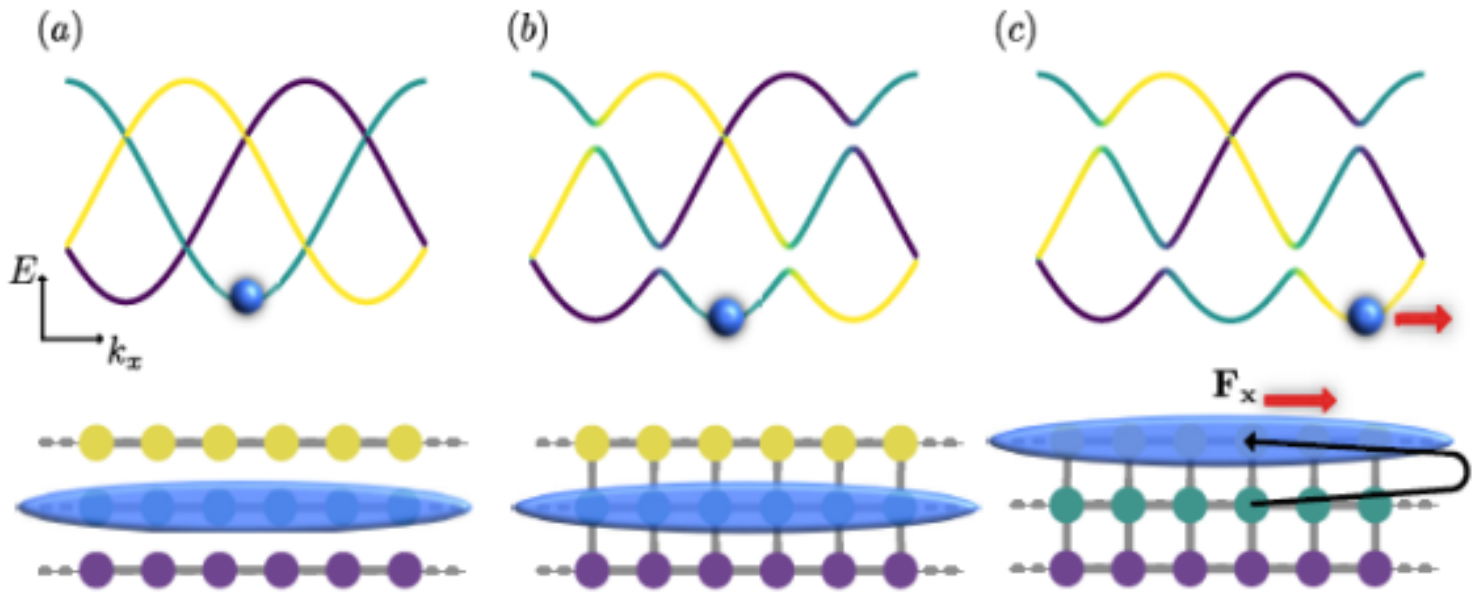


Figure 3: (a) Initially, the Hamiltonian has no tunneling in the $y$ direction. The state is localized at $y = 0$. (b) The tunneling in the $y$ direction is adiabatically turned on, opening gaps in the band structure. (c) Once the adiabatic loading is completed, a force $\mathbf{F_x}$ is applied along $x$, and the wave packet performs Bloch oscillations. The black arrow depicts schematically the motion of the center of mass over the first period of the force. After a complete period, the wave packet returns to the same position along $x$, but it has moved along $y$ of a number of sites proportional to the Chern number of the corresponding energy band.

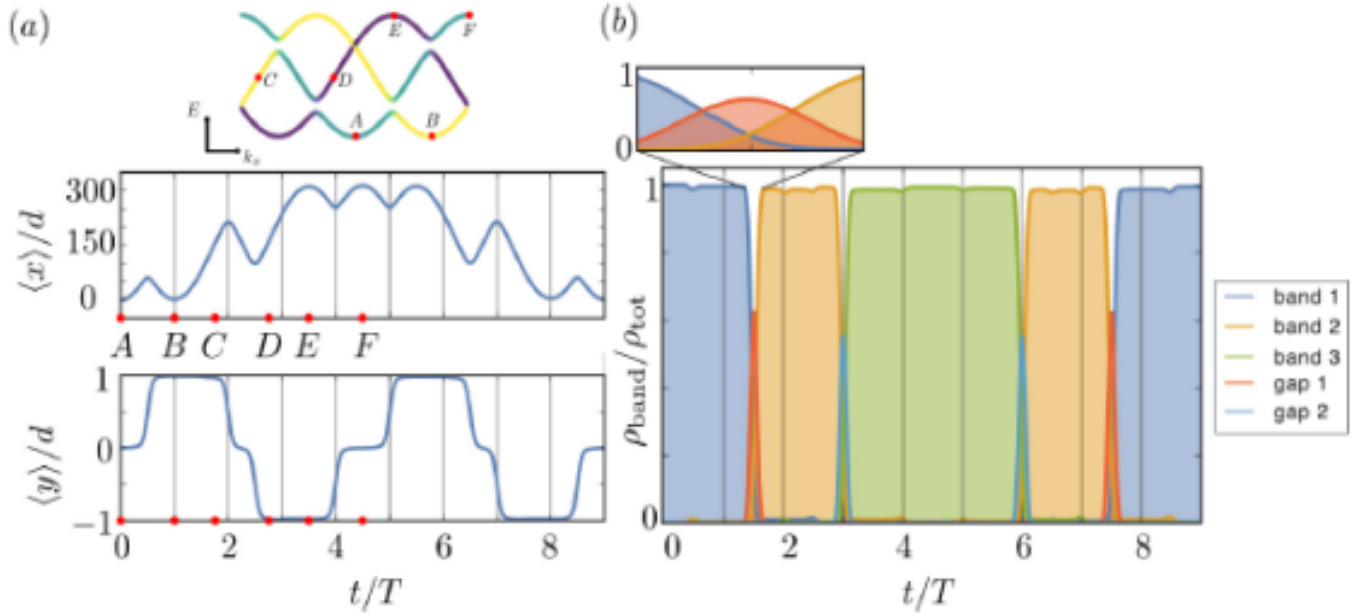


Figure 4: (a) Mean position of the atomic cloud along the $x$ and $y$ directions and (b) populations $\rho$ of bands and band gaps as a function of time, for $J_y = J_x/5$ and $\Phi = \frac{2\pi}{3}$. The red dots labeled $A$–$F$ indicate the corresponding positions in the dispersion relation, as displayed in the inset of (a). The inset of (b) shows a close-up of the populations in the vicinity of the band crossing. Time is measured in units of the period of the force, $T = 2\pi\hbar/(qd|F_x|)$.

arXiv:1804.06345, Imaging topology of Hofstadter ribbons, Dina Genkina, Lauren M. Aycock, Hsin-I Lu, Alina M. Pineiro, Mingwu Lu, I.B. Spielman

SCIENCE ADVANCES | RESEARCH ARTICLE

SOLID STATE PHYSICS

# Probing topology by "heating": Quantized circular dichroism in ultracold atoms

Duc Thanh Tran,[1] Alexandre Dauphin,[2] Adolfo G. Grushin,[3,4] Peter Zoller,[5,6,7] Nathan Goldman[1]*

We reveal an intriguing manifestation of topology, which appears in the depletion rate of topological states of matter in response to an external drive. This phenomenon is presented by analyzing the response of a generic two-dimensional (2D) Chern insulator subjected to a circular time-periodic perturbation. Because of the system's chiral nature, the depletion rate is shown to depend on the orientation of the circular shake; taking the difference between the rates obtained from two opposite orientations of the drive, and integrating over a proper drive-frequency range, provides a direct measure of the topological Chern number ($\nu$) of the populated band: This "differential integrated rate" is directly related to the strength of the driving field through the quantized coefficient $\eta_0 = \nu/h^2$, where $h = 2\pi\hbar$ is Planck's constant. Contrary to the integer quantum Hall effect, this quantized response is found to be nonlinear with respect to the strength of the driving field, and it explicitly involves interband transitions. We investigate the possibility of probing this phenomenon in ultracold gases and highlight the crucial role played by edge states in this effect. We extend our results to 3D lattices, establishing a link between depletion rates and the nonlinear photogalvanic effect predicted for Weyl semimetals. The quantized circular dichroism revealed in this work designates depletion rate measurements as a universal probe for topological order in quantum matter.

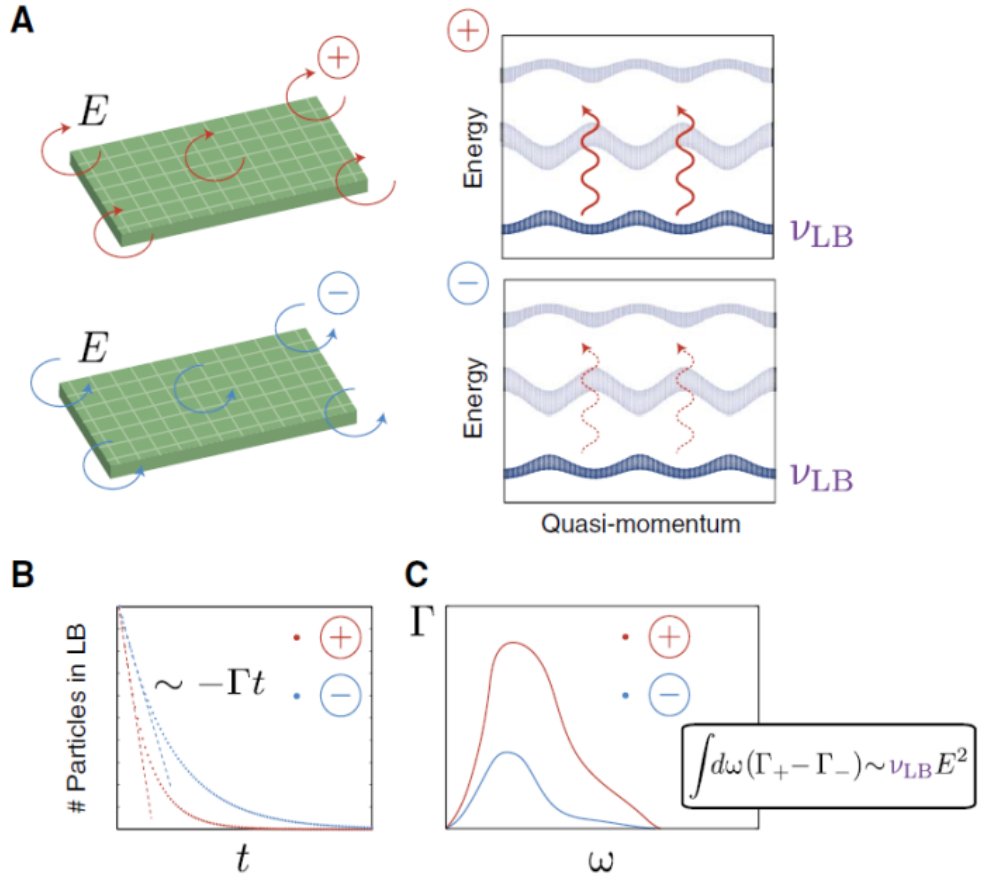


**Fig. 1. Topology through heating.** (**A**) A 2D Fermi gas is initially prepared in the lowest band (LB) of a lattice, with Chern number $\nu_{LB}$, and it is then subjected to a circular time-periodic modulation (Eq. 3). (**B**) The rate $\Gamma$ associated with the depletion of the populated band is found to depend on the orientation of the drive, $\Gamma_+ \neq \Gamma_-$, whenever the LB is characterized by a nontrivial Chern number $\nu_{LB} \neq 0$. (**C**) Integrating the differential rate over a relevant drive-frequency range, $\Delta\Gamma^{int} = \int d\omega(\Gamma_+ - \Gamma_-)/2$, leads to a quantized result, $\Delta\Gamma^{int}/A_{syst} = (\nu_{LB}/h^2)E^2$, where $E$ is the strength of the drive and $A_{syst}$ is the system's area (Eq. 1).

# Conjecture/Open Problem?

PHYSICAL REVIEW A **83**, 013601 (2011)

## Counting of fermions and spins in strongly correlated systems in and out of thermal equilibrium

Sibylle Braungardt,[1,*] Mirta Rodríguez,[2] Aditi Sen(De),[3] Ujjwal Sen,[3] Roy J. Glauber,[4] and Maciej Lewenstein[1,5,6]
[1]*ICFO-Institut de Ciències Fotòniques, Mediterranean Technology Park, E-08860 Castelldefels (Barcelona), Spain*
[2]*Instituto de Estructura de la Materia, CSIC, C/Serrano 121, E-28006 Madrid, Spain*
[3]*Harish-Chandra Research Institute, Chhatnag Road, Jhunsi, Allahabad 211 019, India*
[4]*Lyman Laboratory, Physics Department, Harvard University, 02138 Cambridge, Massachusetts, USA*
[5]*ICREA-Institució Catala de Ricerca i Estudis Avançats, E-08010 Barcelona, Spain*
[6]*Kavli Institute for Theoretical Physics, Kohn Hall, University of California, Santa Barbara, California 93106-4030, USA*
(Received 5 November 2010; published 7 January 2011)

Atom counting theory can be used to study the role of thermal noise in quantum phase transitions and to monitor the dynamics of a quantum system. We illustrate this for a strongly correlated fermionic system, which is equivalent to an anisotropic quantum *XY* chain in a transverse field and can be realized with cold fermionic atoms in an optical lattice. We analyze the counting statistics across the phase diagram in the presence of thermal fluctuations and during its thermalization when the system is coupled to a heat bath. At zero temperature, the quantum phase transition is reflected in the cumulants of the counting distribution. We find that the signatures of the crossover remain visible at low temperature and are obscured with increasing thermal fluctuations. We find that the same quantities may be used to scan the dynamics during the thermalization of the system.

DOI: 10.1103/PhysRevA.83.013601 PACS number(s): 67.85.−d, 05.30.Fk, 75.10.Pq

included in the description.

DOI: 10.1103/PhysRevA.85.033818 PACS number(s): 42.50.Ar, 03.75.Pp, 03.65.Ta

# Loading Ultracold Gases in Topological Floquet Bands: Current and Center-of-Mass Responses

Alexandre Dauphin,[1,*] Duc-Thanh Tran,[2,†] Maciej Lewenstein,[1,3] and Nathan Goldman[2,‡]

[1]*ICFO-Institut de Ciencies Fotoniques, The Barcelona Institute of Science and Technology, 08860 Castelldefels (Barcelona), Spain*
[2]*Center for Nonlinear Phenomena and Complex Systems, Université Libre de Bruxelles, CP 231, Campus Plaine, B-1050 Brussels, Belgium*
[3]*ICREA, Passeig de Lluis Companys 23, E-08010 Barcelona, Spain*

Topological band structures can be designed by subjecting lattice systems to time-periodic modulations, as was recently demonstrated in cold atoms and photonic crystals. However, changing the topological nature of Floquet Bloch bands from trivial to non-trivial, by progressively launching the time-modulation, is necessarily accompanied with gap-closing processes: this has important consequences for the loading of particles into a target Floquet band with non-trivial topology, and hence, on the subsequent measurements. In this work, we analyse how such loading sequences can be optimized in view of probing the topology of Floquet bands through transport measurements. In particular, we demonstrate the robustness of center-of-mass responses, as compared to current responses, which present important irregularities due to an interplay between the micro-motion of the drive and inter-band interference effects. The results presented in this work illustrate how probing the center-of-mass displacement of atomic clouds offers a reliable method to detect the topology of Floquet bands, after realistic loading sequences.

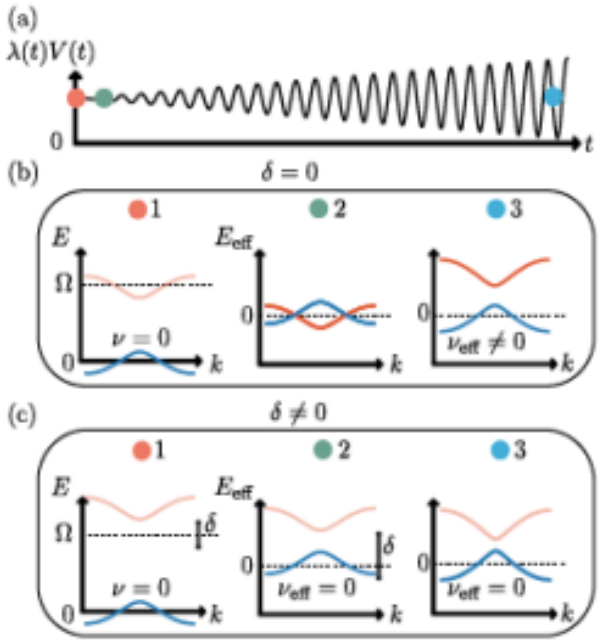


Figure 1. The loading into Floquet bands: Turning on the time-modulation $V(t)$. (a) Sketch of the ramp considered to progressively increase the strength of the time-modulation, $\lambda(t)V(t)$. (b) Illustration of the corresponding (instantaneous) band structure and population: (1) Initially, the lowest band associated with the static Hamiltonian $\hat{H}_0$ is completely filled; the system is topologically trivial, as dictated by the Chern number $\nu = 0$ of the populated band; the two bands are separated by a gap of order $\Omega$ due to the offset between $A$ and $B$ sites [Eq. (6)]; (2) As soon as the time-modulation is turned on, the band structure is described in terms of instantaneous Floquet bands, $E_{\rm eff}$, which are defined modulo $\Omega$; in this picture, the bands strongly overlap, thus leading to severe band repopulation during the early stage of the ramp [$\lambda(t) \approx 0$]; (3) At the end of the ramp, the Floquet bands are topologically non-trivial, as marked by non-zero Chern numbers $\nu_{\rm eff} \neq 0$; here, both Floquet bands (with opposite Chern numbers) are largely populated, indicating the inefficiency of this scheme to prepare the system in the lowest Floquet band only. (c) Same protocol as for (b), except that a detuning $\delta$ has been introduced [Eq. (6)] so as to avoid any overlap between the Floquet bands during the entire ramp $\lambda(t)V(t)$; at the end of the sequence, only the lowest band is occupied; in this case, the populated Floquet band has a trivial topology $\nu_{\rm eff} = 0$, due to the large detuning $\delta$. A controlled transition, from trivial to non-trivial Floquet bands, can then be induced by removing the detuning; see Fig. 2.

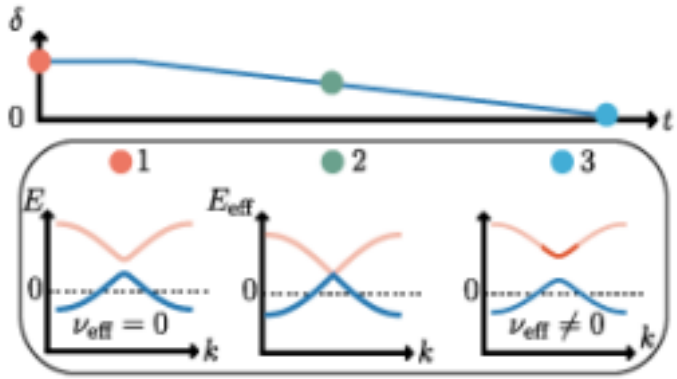


Figure 2. The second step of the loading sequence. As the detuning is progressively decreased, the Floquet bands introduced in Fig. 1(c) undergo a controlled topological phase transition, leading to a limited excited fraction in the upper band. At the end of the sequence, most of the particles occupy the lowest Floquet band, with non-zero Chern number $\nu_{\rm eff} \neq 0$. This second step of the loading protocol can be optimized by increasing the duration of the ramp $\delta(t)$, i.e. by minimizing Landau-Zener transitions during the gap closing event; see also Eq. (29).

### A. Time-dependent Hamiltonian and effective flat-band model

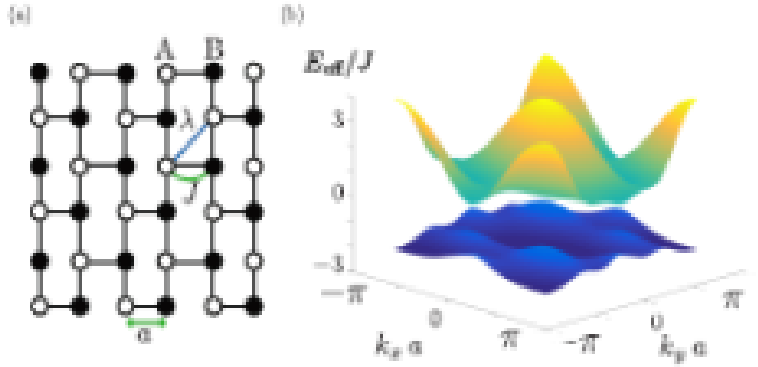


Figure 3. (a) Sketch of the brickwall lattice and its NN and NNN links (with hopping parameters $J$ and $\lambda$, respectively). (b) Energy spectrum associated with effective Hamiltonian in Eq. (B11), in the absence of detuning $\delta = 0$. The other system parameters satisfy $J_{ij}^{\rm eff} = J$, $\lambda_{ij}^{\rm eff} = 0.3J$ and $\mathbf{q} = (6,2)/a$. The lowest quasi-flat band is separated from the higher band by a gap $\Delta_{\rm gap} = 1.73J$, and it is topologically non-trivial, with Chern number $\nu_{\rm tot} = 1$.

#### 1. *Dynamics under the effective Hamiltonian: Neglecting the micro-motion*

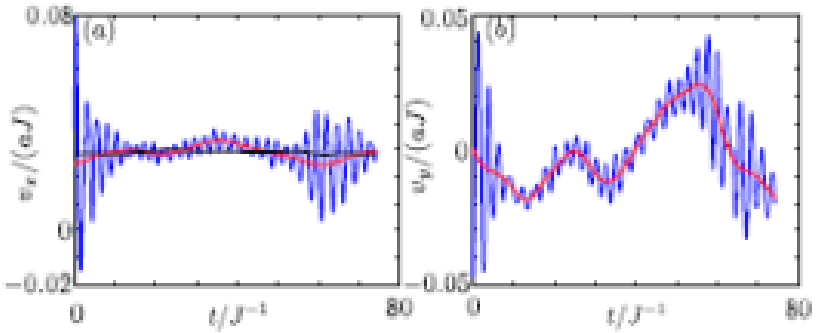


Figure 8. Velocity of the center of mass (blue line) along the $x$ and $y$ directions, as computed using the full equations of motion (18)-(19). Removing the contribution of the inter-band velocity term [Eq. (17)] leads to a smoother behavior (red curve). The isolated contribution of the anomalous velocity [Eq. (16)] is shown in black.

# Simulating a Chern insulator with a photonic 2D quantum walk

*Two-dimensional topological quantum walks in the momentum space of structured light*,
A. D'Errico, F. Cardano, **M.M.**, A. Dauphin, R. Barboza, C. Esposito, B. Piccirillo, M. Lewenstein, P. Massignan, L. Marrucci,
arXiv preprint arXiv:1811.04001 (2018)

# Integer Quantum Hall effect on the lattice

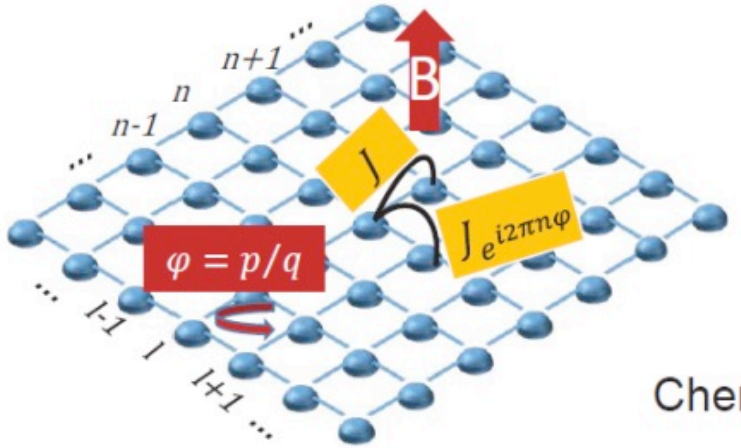


Hofstadter model

- Non-interacting electrons
- Uniform magnetic field
- Rational magnetic flux through the cell

Chern number of the n-th energy band

$$\nu^{(n)} = \frac{1}{2\pi}\iint_{\text{R.B.Z.}} d^2k\, \Omega_{xy}{}^{(n)}$$

$$\Omega_{xy}{}^{(n)} = \left\langle \frac{\partial u_{\boldsymbol{k}}{}^{(n)}}{\partial k_x} \middle| \frac{\partial u_{\boldsymbol{k}}{}^{(n)}}{\partial k_y} \right\rangle - \left\langle \frac{\partial u_{\boldsymbol{k}}{}^{(n)}}{\partial k_y} \middle| \frac{\partial u_{\boldsymbol{k}}{}^{(n)}}{\partial k_x} \right\rangle$$

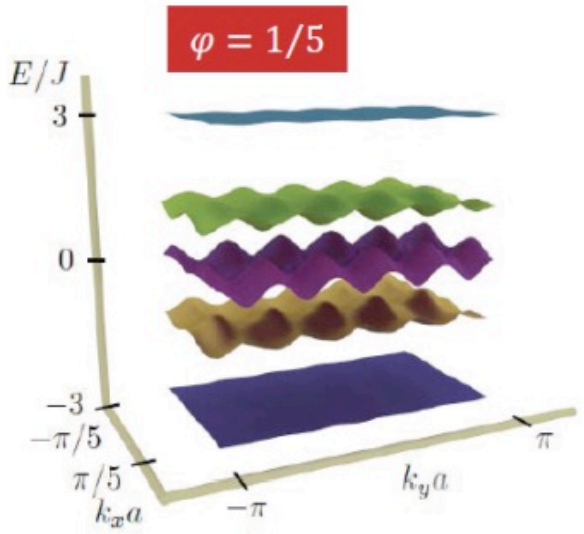


$\nu^{(5)} = 1$

$\nu^{(4)} = 1$

$\nu^{(3)} = -4$

$\nu^{(2)} = 1$

$\nu^{(1)} = 1$


D. R. Hofstadter, *Phys. Rev. B* **14**: 2239 (1976)

D. J. Thouless, M. Kohmoto, M. P. Nightingale, and M. den Nijs, Phys. Rev. Lett. **49**: 405 (1982)

# Integer Quantum Hall effect on the lattice

The Hall conductivity in each gap is proportional to the Chern number of the bands below

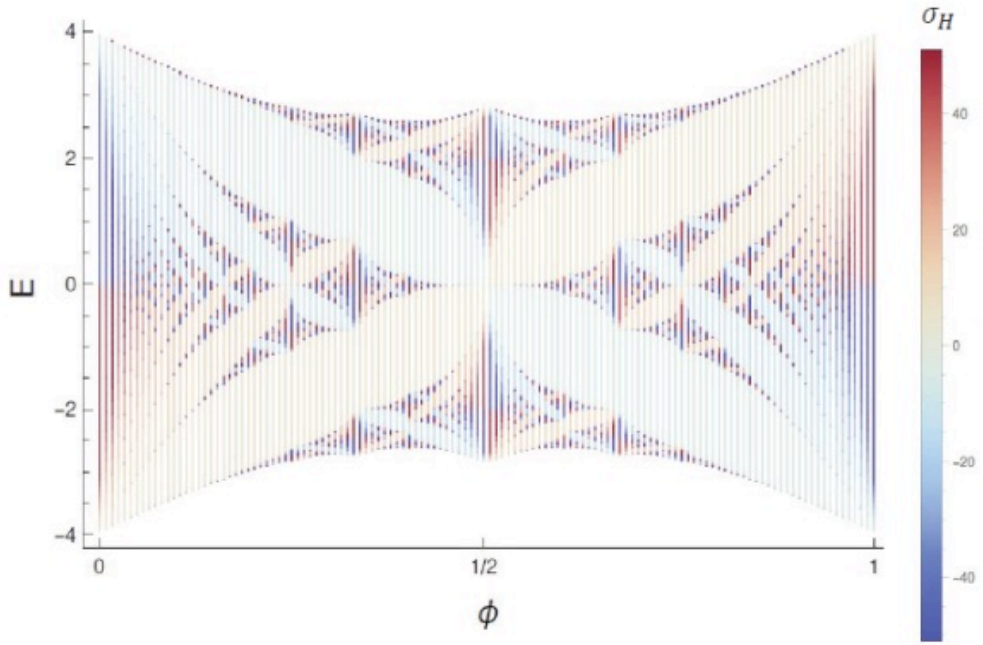

# Quantum Walk with light's transverse wavevector

- The walker position is the transverse wavevector of a light beam
- The coin is its polarization

$$|\boldsymbol{m}\rangle \otimes |s\rangle = A(\boldsymbol{r}) e^{i[\Delta k_\perp (m_x x + m_y y) + k_z z]} \otimes \left(\alpha|R\rangle + \beta|L\rangle\right) \qquad \Delta k_\perp \ll k_z \approx |k|$$

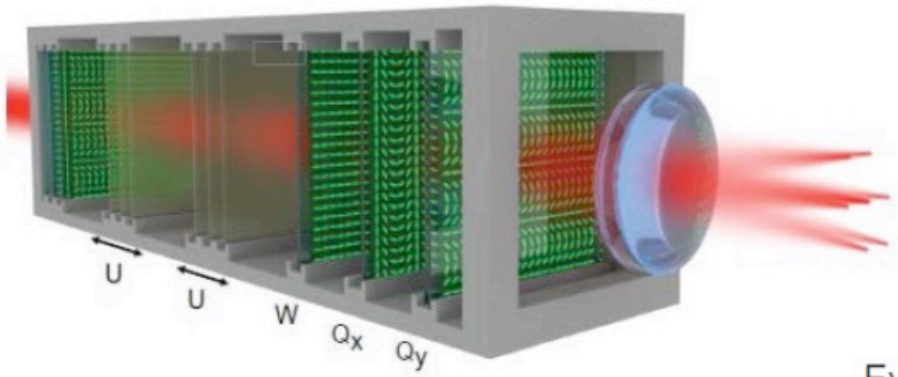


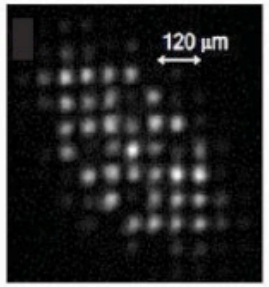


Every site of the 2D effective lattice is a spot in the focal plane of a lens placed at the exit of the QW

A. D'Errico, F. Cardano, **M. M.**, A. Dauphin,…, M. Lewenstein, P. Massignan, L. Marrucci, arXiv:1811.04001 (2018)

# Quantum Walk with light's transverse wavevector

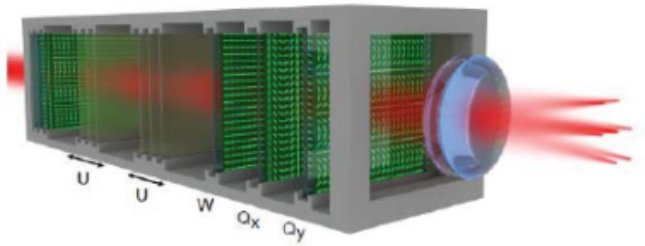


$$U = Q_y(\delta) \cdot Q_x(\delta) \cdot W$$

$$W = \begin{pmatrix} 1/\sqrt{2} & i/\sqrt{2} \\ i/\sqrt{2} & 1/\sqrt{2} \end{pmatrix}$$

Quarter-wave plate:
Polarization rotation

$$Q_x(\delta) = \begin{pmatrix} \cos\left(\frac{\delta}{2}\right) & isin\left(\frac{\delta}{2}\right)e^{-ik_x} \\ isin\left(\frac{\delta}{2}\right)e^{ik_x} & \cos\left(\frac{\delta}{2}\right) \end{pmatrix}$$

G-plate:
Polarization dependent diffraction grating

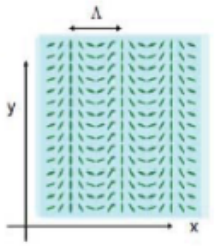


$$\frac{2\pi}{\Lambda} = \text{lattice spacing}$$

A. D'Errico, F. Cardano, **M. M.**, A. Dauphin,…, M. Lewenstein, P. Massignan, L. Marrucci, arXiv:1811.04001 (2018)

# Quantum Walk with light's transverse wavevector

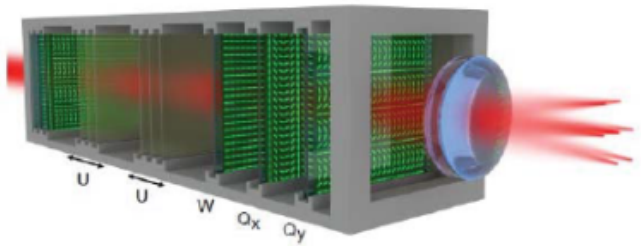


$$U = Q_y(\delta) \cdot Q_x(\delta) \cdot W$$

$$i \log U(\boldsymbol{k}) = H_{eff}(\boldsymbol{k}) = \varepsilon(\boldsymbol{k})\mathbf{n}(\boldsymbol{k}) \cdot \boldsymbol{\sigma}$$

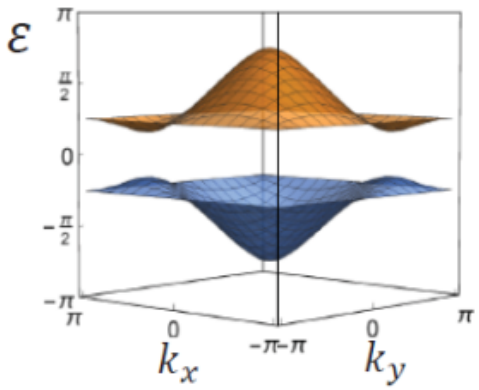


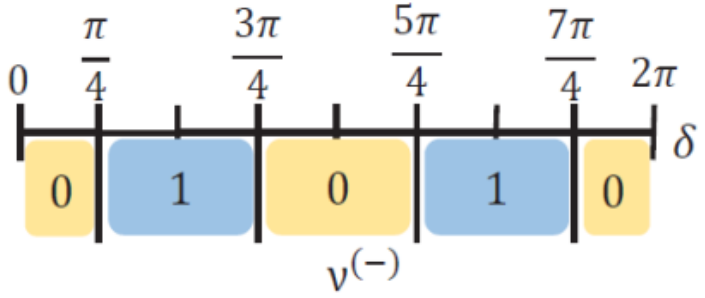


Topological quantum walk protocol

A. D'Errico, F. Cardano, **M. M.**, A. Dauphin,…, M. Lewenstein, P. Massignan, L. Marrucci, arXiv:1811.04001 (2018)

# Measuring Chern numbers through transverse displacements

Adiabatic semiclassical EOM of a wavepacket centred on an energy eigenstate

$$\dot{m}_i^{(n)} = \mathrm{vg}_i^{(n)} + F^j \Omega_{ji}^{(n)}$$

group velocity — Berry curvature

Overall band displacement with $\boldsymbol{F} = (F_x, 0)$:

$$\langle \Delta m_y \rangle^{(n)} = \frac{F_x \nu^{(n)} t}{2\pi} \,, \quad \langle \Delta m_x \rangle^{(n)} = 0$$

D.Xiao et al., *Rev. Mod. Phys.*, **82**:1959 (2010)
H.M.Price et al., *Phys. Rev. B*, **93**: 245113 (2016)

Realized in several simulators with ultracold bosons and fermions

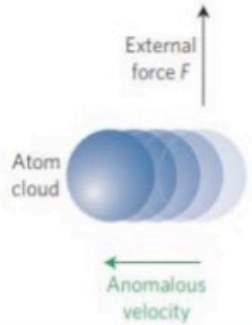


M. Aidelsburger et al., *Nat. Phys.* **11**:162 (2015)

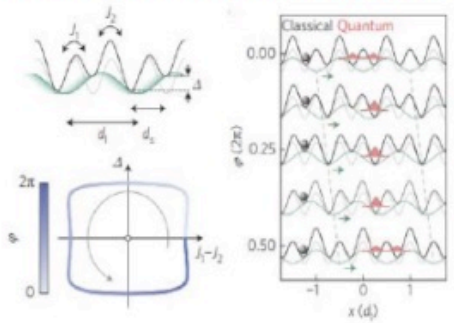


M. Lohse et al., *Nat. Phys.* **12**:350 (2015)

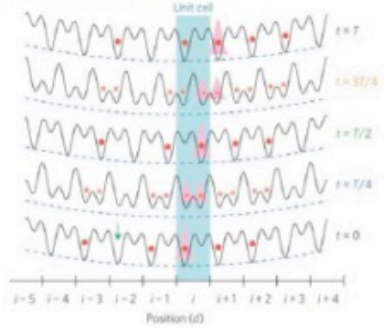

S. Nakajima et al., *Nat. Phys.***12**:296 (2016)

# Wavepackets dynamics

It is possible to prepare a wavepacket in a specific energy and momentum state

With $\boldsymbol{F} = 0$

$$\dot{m}_i{}^{(+)} = \mathrm{vg}_i{}^{(+)}$$

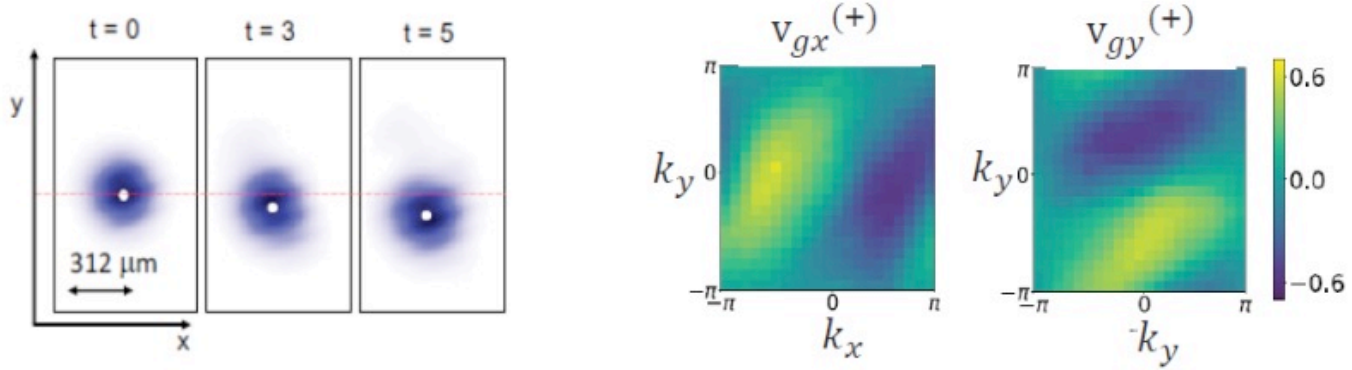


A. D'Errico, F. Cardano, **M. M.**, A. Dauphin,..., M. Lewenstein, P. Massignan, L. Marrucci, arXiv:1811.04001 (2018)

# Wavepackets dynamics

It is possible to prepare a wavepacket in a specific energy and momentum state

With $\boldsymbol{F} = (F_x, 0)$

$$\langle \Delta m_y \rangle^{(-)} = \frac{F_x v^{(-)} t}{2\pi}, \langle \Delta m_x \rangle^{(-)} = 0$$

$F_x = \pi/20$

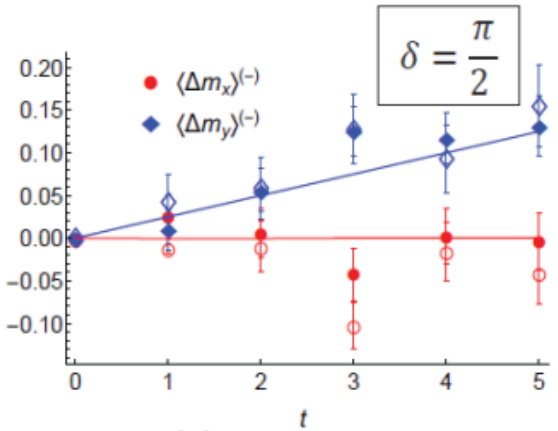


$v^{(-)} = 1.19 \pm 0.13$

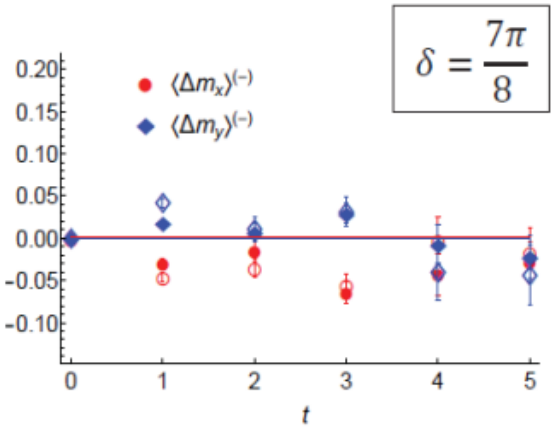


$v^{(-)} = 0.10 \pm 0.15$

A. D'Errico, F. Cardano, **M. M.**, A. Dauphin,..., M. Lewenstein, P. Massignan, L. Marrucci, arXiv:1811.04001 (2018)

# 3. Detection of topological order in 1D interacting systems

ICFO The Institute of Photonic Sciences

INTERNATIONAL YEAR OF LIGHT 2015

*iCrea

INSTITUCIÓ CATALANA DE RECERCA I ESTUDIS AVANÇATS

# Strongly Correlated Bosons on a Dynamical Lattice

Daniel González-Cuadra,[1] Przemysław R. Grzybowski,[1,2] Alexandre Dauphin,[1] and Maciej Lewenstein[1,3]
[1]*ICFO-Institut de Ciències Fotòniques, The Barcelona Institute of Science and Technology, Av. Carl Friedrich Gauss 3, 08860 Barcelona, Spain*
[2]*Faculty of Physics, Adam Mickiewicz University, Umultowska 85, 61-614 Poznań, Poland*
[3]*ICREA, Passeig Lluís Companys 23, 08010 Barcelona, Spain*

(Received 23 February 2018; published 30 August 2018)

We study a one-dimensional system of strongly correlated bosons on a dynamical lattice. To this end, we extend the standard Bose-Hubbard Hamiltonian to include extra degrees of freedom on the bonds of the lattice. We show that this minimal model exhibits phenomena reminiscent of fermion-phonon models. In particular, we discover a bosonic analog of the Peierls transition, where the translational symmetry of the underlying lattice is spontaneously broken. This provides a dynamical mechanism to obtain a topological insulator in the presence of interactions, analogous to the Su-Schrieffer-Heeger model for electrons. We characterize the phase diagram numerically, showing different types of bond order waves and topological solitons. Finally, we study the possibility of implementing the model using atomic systems.

DOI: 10.1103/PhysRevLett.121.090402

# Fermion-Lattice effects in 1D: Peierls' Transition

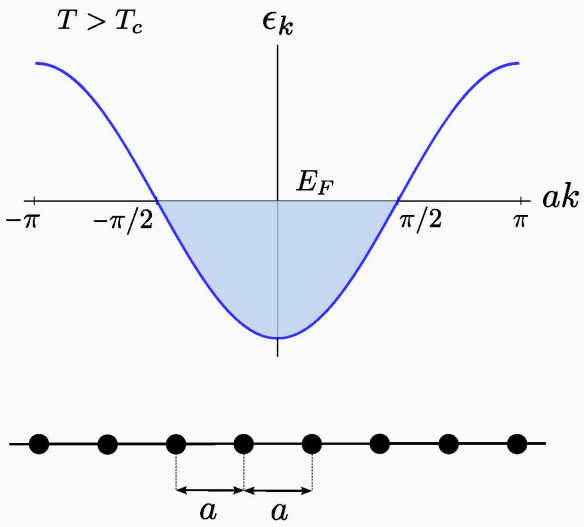


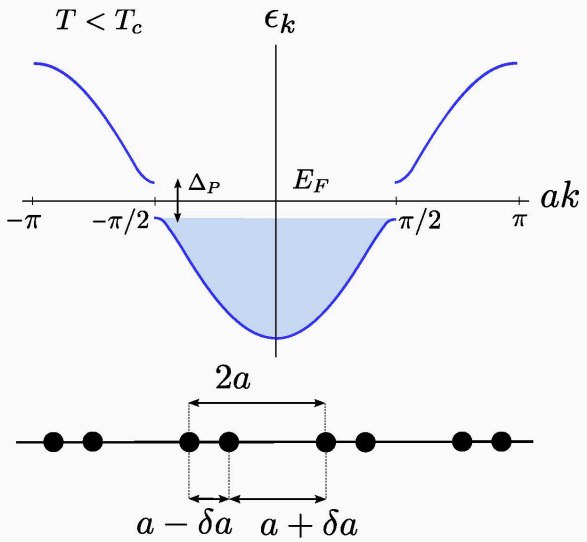


## Peierls' Theorem (1955)

A 1D equally spaced chain with one electron per ion is unstable

**E.g. Polyacetylene**

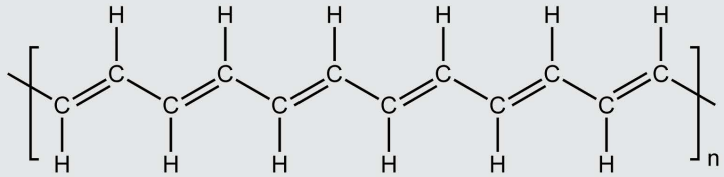


## Su-Schrieffer-Heeger Model

Su *et al*, Phys. Rev. Lett. (1979)

$$\hat{H} = \sum_i \left( \frac{\hat{P}_i^2}{2M} + K(\hat{u}_{i+1} - \hat{u}_i)^2 \right)$$
$$- \sum_{i,\sigma} (t - \alpha(\hat{u}_{i+1} - \hat{u}_i)) (\hat{c}^\dagger_{i,\sigma} \hat{c}_{i+1,\sigma} + \text{H.c})$$

# Motivations

Simon Wall



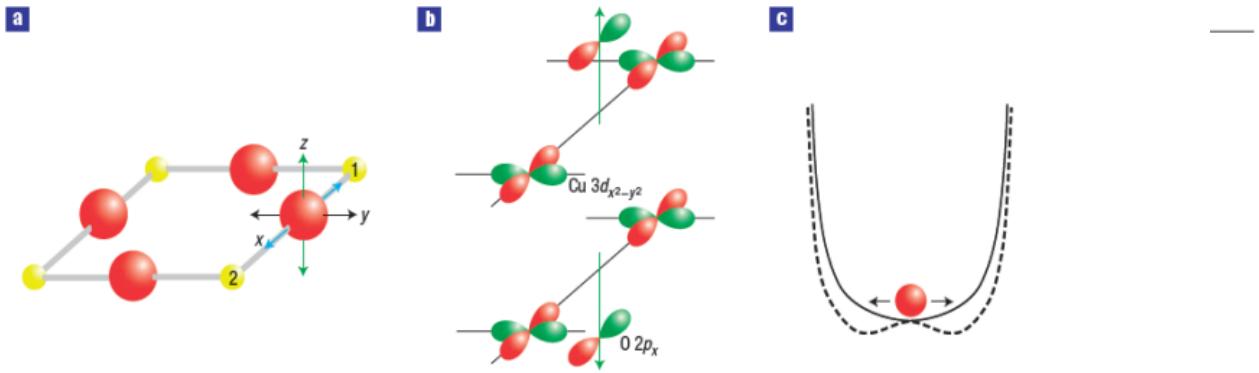


**Figure 1 Oxygen degrees of freedom and electron–phonon coupling. a**, The unit cell in the $CuO_2$ plane, with Cu atoms (yellow) and O atoms (red), showing $x$, $y$ and $z$ vibrational modes (arrows). **b**, The Cu $3d_{x^2-y^2}$ and O $2p_x$ orbitals, illustrating the effect of an O $z$ displacement (green arrows), positive sense (top panel) and negative sense (bottom panel). **c**, Bare oxygen anharmonic potential (3): full (dashed) curves with positive (negative) harmonic coefficient $\chi$ in equation (3).

Hence the electron–vibrator term in the hamiltonian must have the unusual second-order form of coupling

$$h_{12}^{ev} = \frac{\nu}{2} z^2 \sum_{\sigma} \left( c_{1,\sigma}^{+} c_{2,\sigma} + c_{2,\sigma}^{+} c_{1,\sigma} \right), \qquad (2)$$

anharmonic vibrator hamiltonian should have the form

$$h_{12}^{v} = \frac{p_z^2}{2m} + \frac{\chi}{2} z^2 + \frac{w}{8} z^4, \qquad (3)$$

ides a critical temperature $T_c$ of the order of 100 K, they include a $d$-wave superconducting
s, a pseudogap with $d$-symmetry and the characteristic temperature scale $T^*$, an anomalous

doping-dependent oxygen isotope
vibrations, but conventional Bard
on-site Coulomb interaction $U$. H
liquid nature of the $d$-wave super
fluctuations are manifested in a pa
On the basis of such bond fluctuat

Here the electronic term includes hopping over longer ranges than the nearest-neighbour hopping considered in equation (1):

$$H^{e} = -\frac{1}{2} \sum_{i,j,\sigma} t(i-j)\, c_{i,\sigma}^{+} c_{j,\sigma}, \qquad (6)$$

Leticia Tarruell

# Strongly Correlated Bosons on a Dynamical Lattice

Daniel González-Cuadra, P. R. Grzybowski, A. Dauphin, M. Lewenstein, arXiv:1802.05689 (2018) (accepted PRL)

$$\hat{H} = -t\sum_i \left(\hat{b}_i^\dagger \hat{b}_{i+1} + h.c.\right) + \frac{U}{2}\sum_i \hat{n}_i(\hat{n}_i - 1) - \mu\sum_i \hat{n}_i$$
$$-\alpha\sum_i \left(\hat{b}_i^\dagger \hat{\sigma}_i^z \hat{b}_{i+1} + h.c.\right) + \frac{\Delta}{2}\sum_i \hat{\sigma}_i^z + \beta\sum_i \hat{\sigma}_i^x$$

- Simplified dynamical lattice: set of spins
- Fermions: $U \to \infty$ (recover SSH physics)

## Bosonic Peierls Transition

For sufficiently strong boson interactions, the dynamical lattice rearranges in a pattern that depends on the bosonic density.

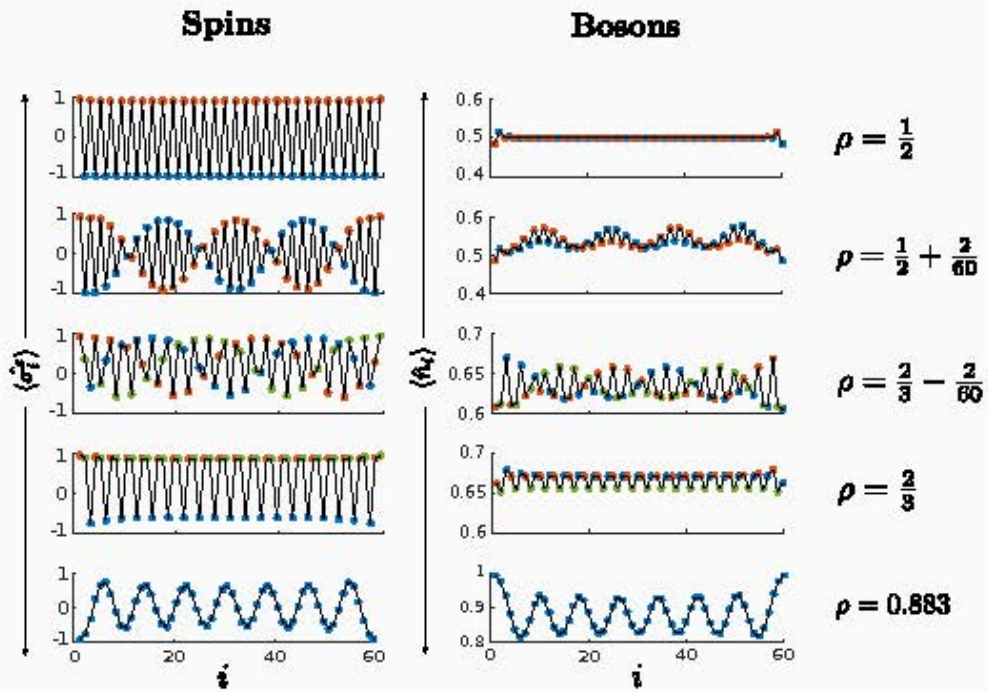

# Characterization of Quantum Phases

**Structure factor:**

$$S(k) = \frac{1}{L} \sum_{i,j} e^{(x_i - x_j)ki} \langle \hat{\sigma}_i^z \hat{\sigma}_j^z \rangle$$

**Compressibility:** $\kappa = \frac{\partial \rho}{\partial \mu}$

**Order wavelength:** $\lambda_0 = \frac{2\pi}{k_0}$

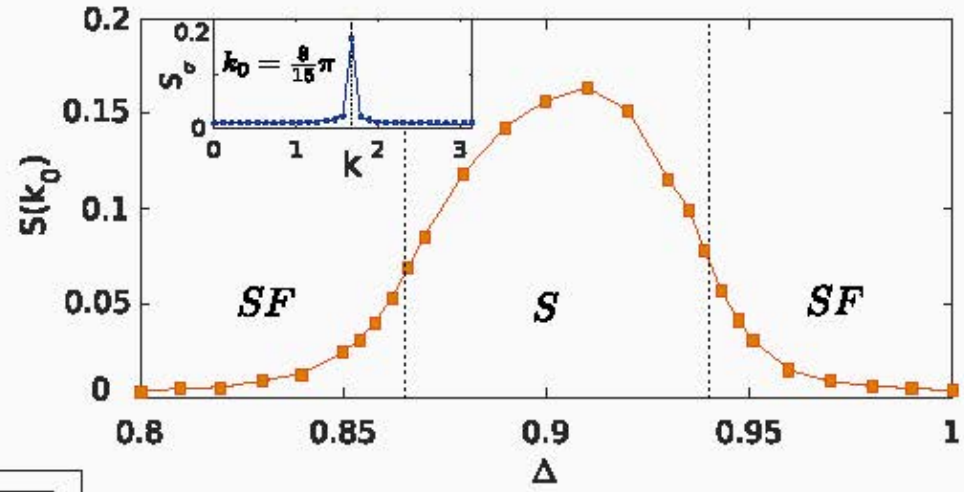


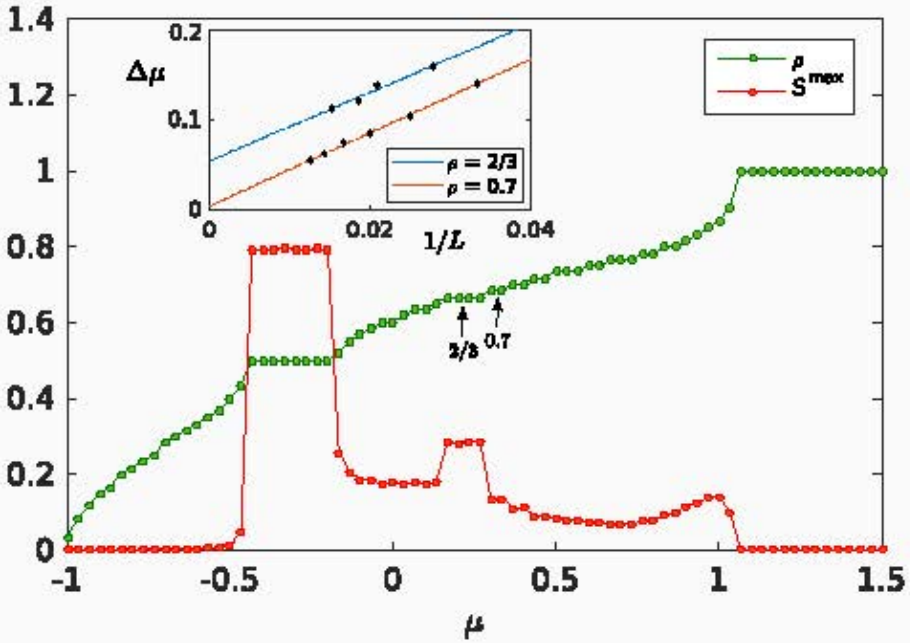


- Commensurate bond order wave (cBOW): $S \neq 0$, $\kappa = 0$, $\lambda_0 \in \mathbb{N}$
- Incommensurate bond order wave (iBOW): $S \neq 0$, $\kappa \neq 0$, $\lambda_0 \notin \mathbb{N}$
- Superfluid (SF): $S = 0$, $\kappa \neq 0$
- Mott Insulator (MI): $S = 0$, $\kappa = 0$

# Phase diagram

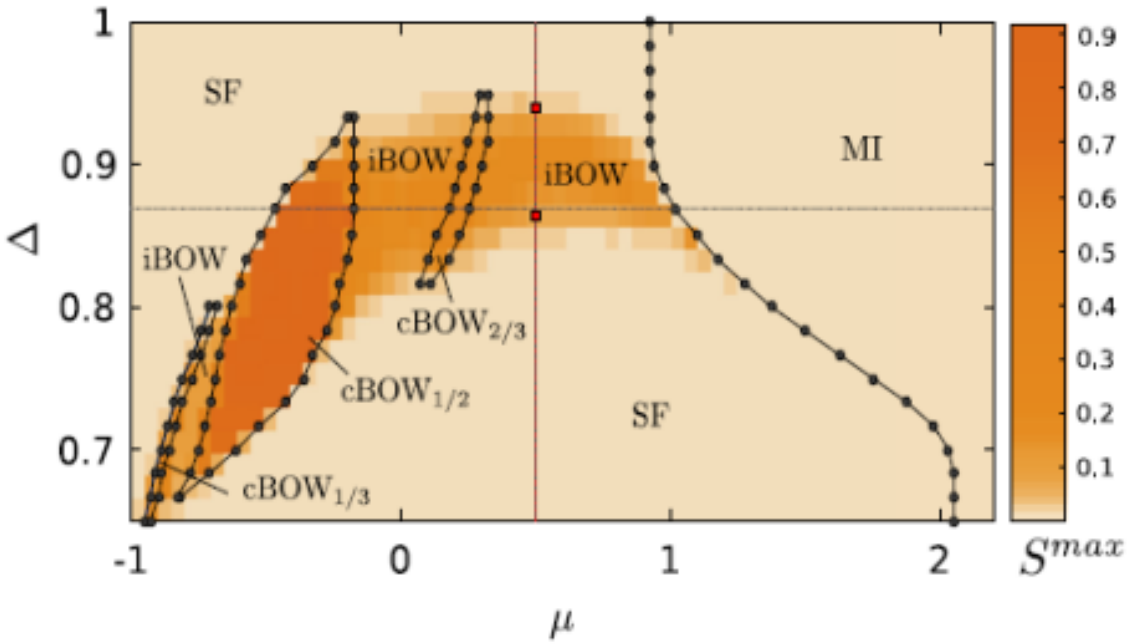


FIG. 4. Phase diagram of the Hamiltonian (1) for a system size of $L = 60$ in terms of $\Delta$ and $\mu$. The solid black lines delimit the incompressible phases (cBOW and MI). The maximum value of the structure factor is represented by the color plot, qualitatively distinguishing between the iBOW and SF phases. The dotted lines correspond to the cuts for $\mu = 0.5$ (Fig. 2) and $\Delta = 0.87$ (Fig. 3). For the former, the red squares mark two critical points in the thermodynamic limit.

# $\mathbb{Z}_2$ Bose-Hubbard Model

**Half Filling:** $\rho = 1/2$

# $\mathbb{Z}_2$ Bose-Hubbard Model

D. González-Cuadra *et al*, Phys. Rev. Lett. **121**, 090402 (2018)

D. González-Cuadra *et al*, Phys. Rev. B **99**, 045139 (2019)

$$\hat{H} = -t \sum_i \left( \hat{b}_i^\dagger \hat{b}_{i+1} + h.c. \right) + \frac{U}{2} \sum_i \hat{n}_i (\hat{n}_i - 1)$$

$$- \alpha \sum_i \left( \hat{b}_i^\dagger \hat{\sigma}_{i,i+1}^z \hat{b}_{i+1} + h.c. \right) + \frac{\Delta}{2} \sum_i \hat{\sigma}_{i,i+1}^z + \beta \sum_i \hat{\sigma}_{i,i+1}^x$$

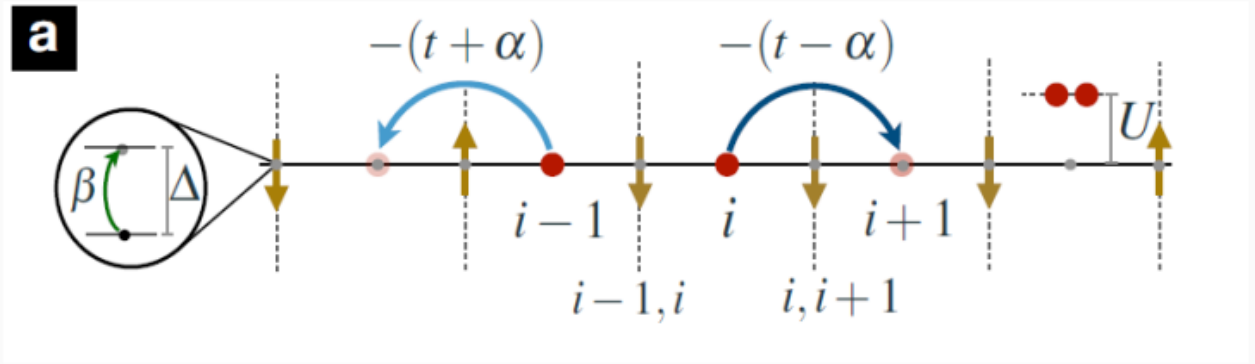

# Bond Order Wave (BOW)

**Jordan-Wigner transformation (For $U \to \infty$, $\beta = 0$)**

$$\hat{H} = -\sum_i \left[\hat{c}_i^\dagger (t + \alpha\hat{\sigma}_i^z)\hat{c}_{i+1} + \text{h.c.}\right] + \frac{\Delta}{2}\sum_i \hat{\sigma}_i^z$$

- Metallic phase
  $\Delta = 0$, $\Delta \gg \alpha$
- Bond Order Wave
  $\Delta_c^- < \Delta < \Delta_c^+$

$$\Delta_c^\pm = \frac{4t}{\pi}\left[\frac{\alpha}{t} \pm \left(E\left(1 - \frac{\alpha^2}{t^2}\right) - 1\right)\right]$$

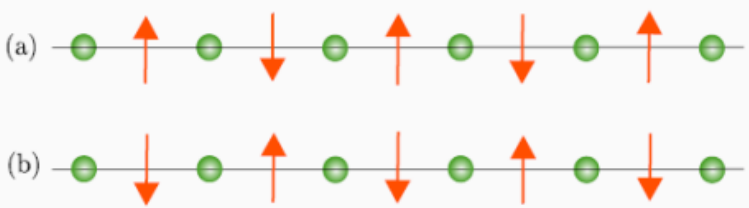


- Two degenerate states:
  (a) trivial and (b) topological
- Survives for $\beta > 0$ and finite $U$
  (**Bosonic Peierls Transition**)

# Topological Signatures

## Local Berry Phase

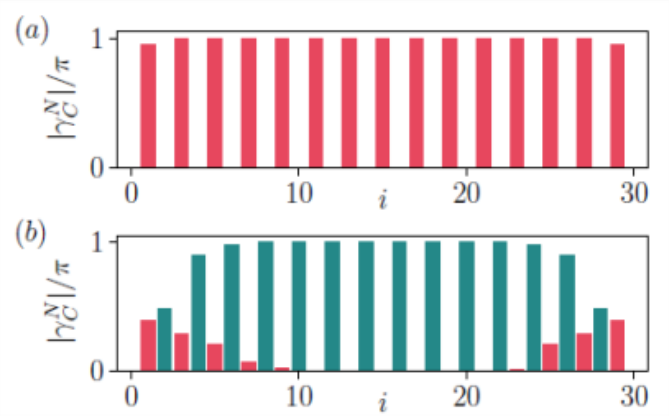


$$\gamma_C = i \oint_C \mathrm{d}\lambda \, \langle \psi(\lambda) | \partial_\lambda \psi(\lambda) \rangle$$

- Local perturbation: $t_{j,j+1} = te^{i\lambda}$

## Many-body edge states

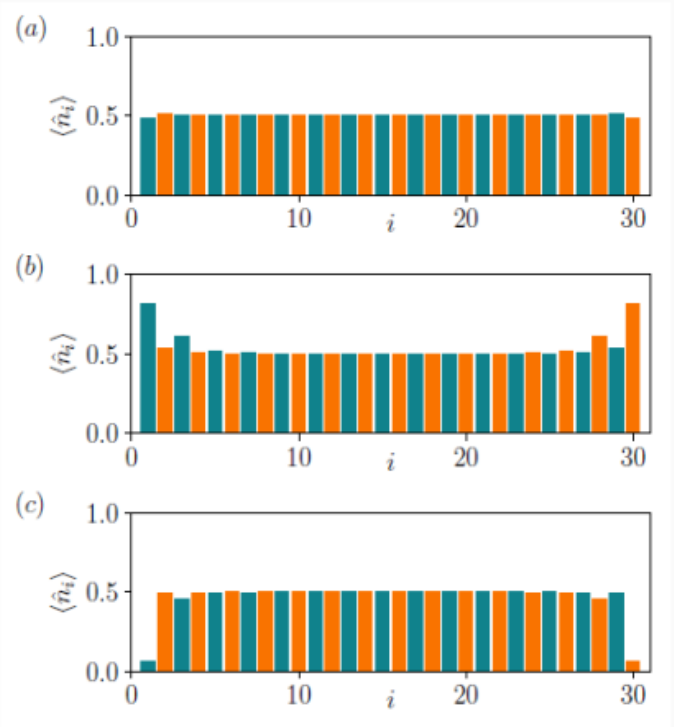


**(a)** Trivial BOW

**(b), (c)** Topological BOW

# Phase diagram

## Topological Bond Order Wave

Interaction-induced symmetry-broken topological insulator

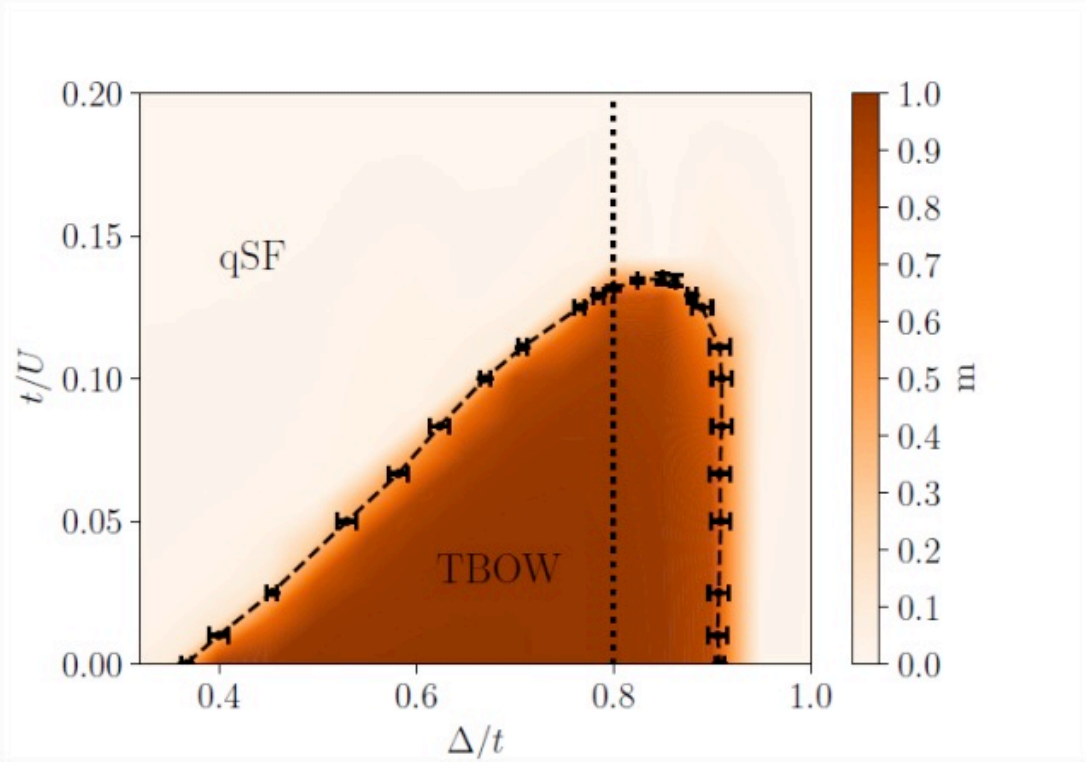


$$m = \sum_i (-1)^i \langle \sigma_{i,i+1} \rangle$$

## $\mathbb{Z}_2$ Bose-Hubbard Model

**Fractional fillings:** $\rho = 1/3$, $\rho = 2/3$

# TBOW$_{2/3}$

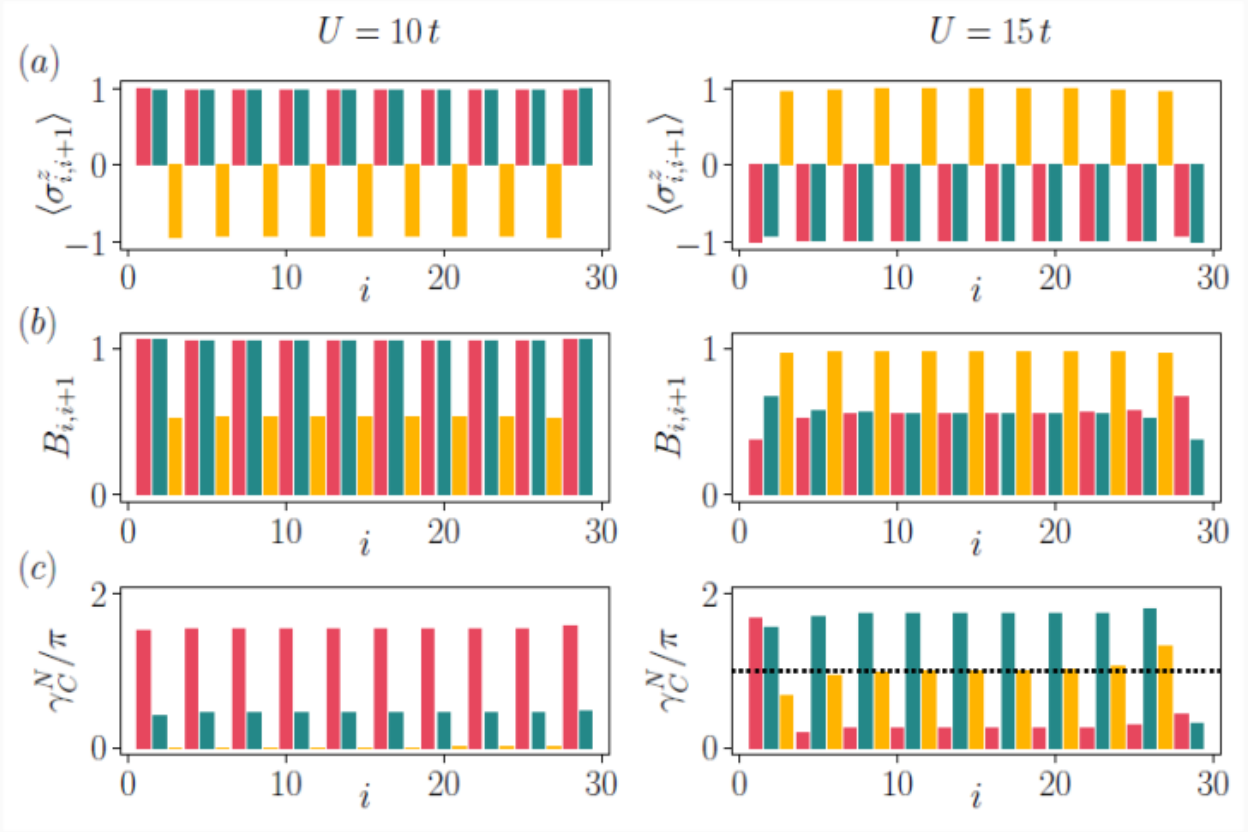


$$B_{i,i+1} = \langle \hat{b}_i^\dagger \hat{b}_{i+1} + \text{H.c.} \rangle$$

# Topological Phase Transitions

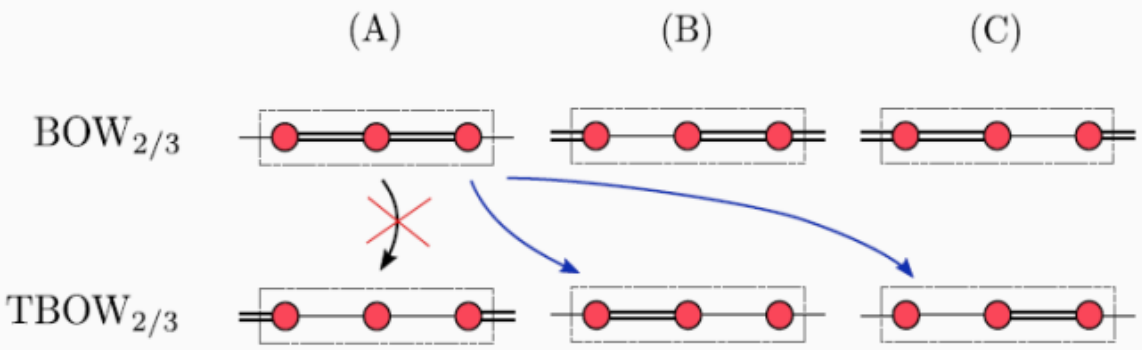

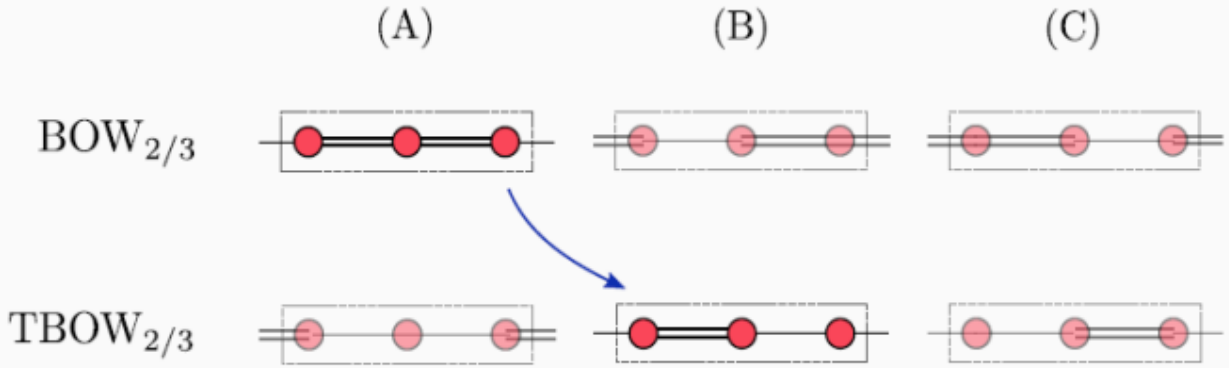


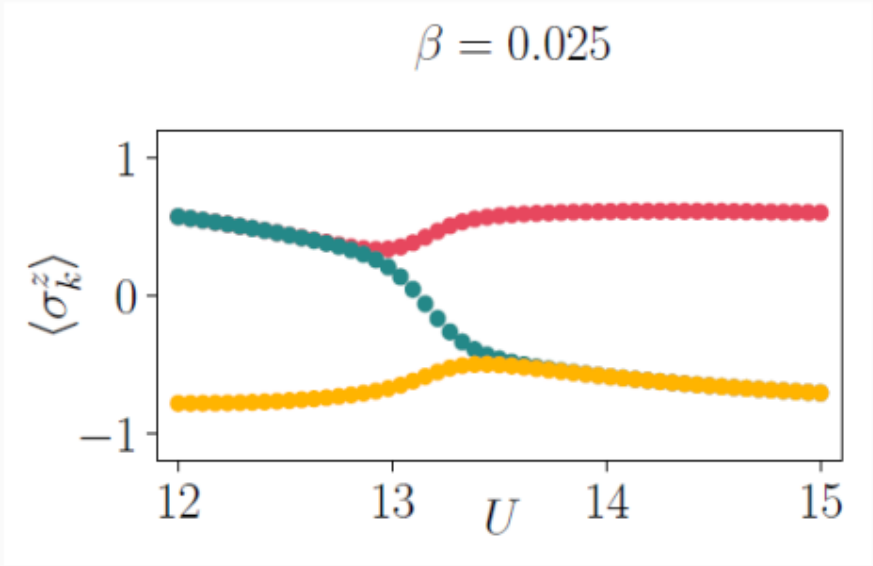


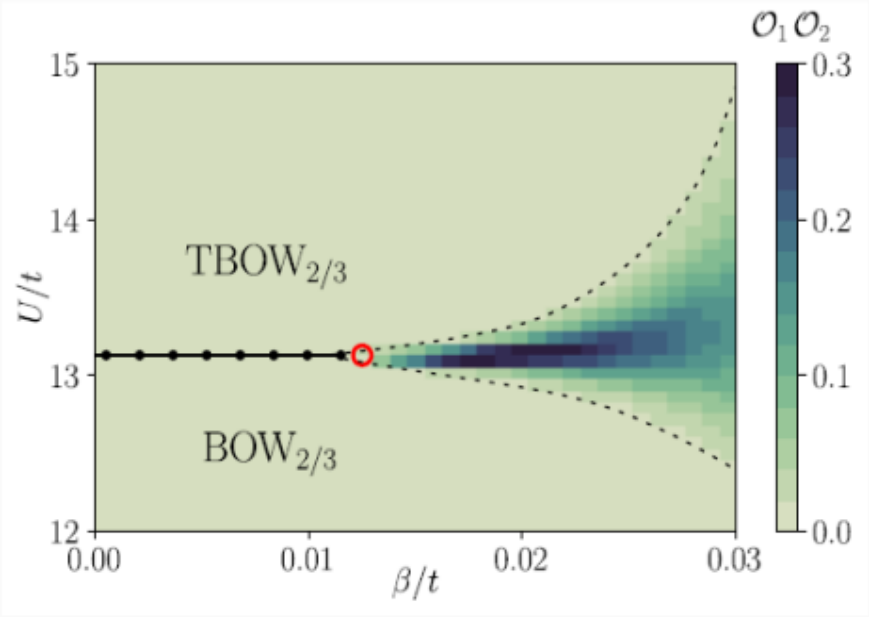


$$\mathcal{O}_1\mathcal{O}_2 = \langle \sigma_1^z - \sigma_2^z \rangle \langle \sigma_2^z - \sigma_3^z \rangle$$

# Self-Adjusting Pumping

## Topology Detection

# Thouless Pumping

## Archimedes's screw

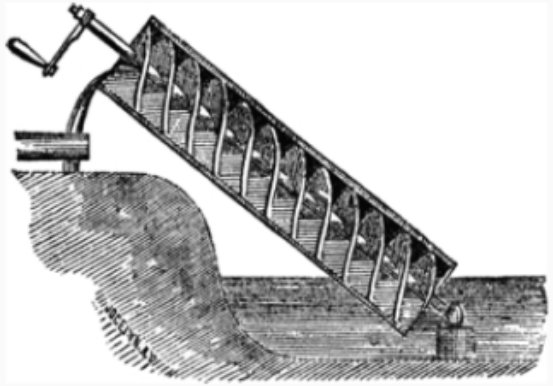

## Quantum Pumping

The integrated particle current produced by a slow periodic variation of the potential of a Schrödinger equation in an infinite periodic system with full bands must have an integer value. Thouless, Phys. Rev. B 27, 6083 (1983)

## Rice-Mele model

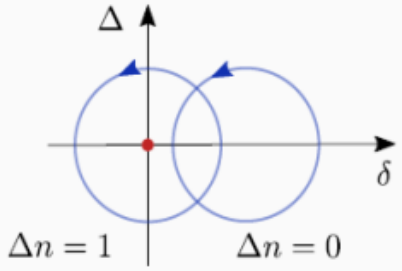


$$\Delta n = -\frac{1}{2\pi}\sum_n \int_0^T \mathrm{d}t \int_{\mathrm{BZ}} \mathrm{d}q\, \Omega^n_{qt}$$

$$\Omega^n_{qt} = i\left(\langle \partial_q u_n | \partial_t u_n\rangle - \langle \partial_t u_n | \partial_q u_n\rangle\right)$$

$$\hat{H} = -\sum_i \left([t + \delta\cos(\varphi)(-1)^i]\hat{c}_i^\dagger \hat{c}_{i+1} + \mathrm{H.c.}\right) + \Delta\sin(\varphi)\sum_i (-1)^i \hat{n}_i$$

# Self-Adjusted Pumping

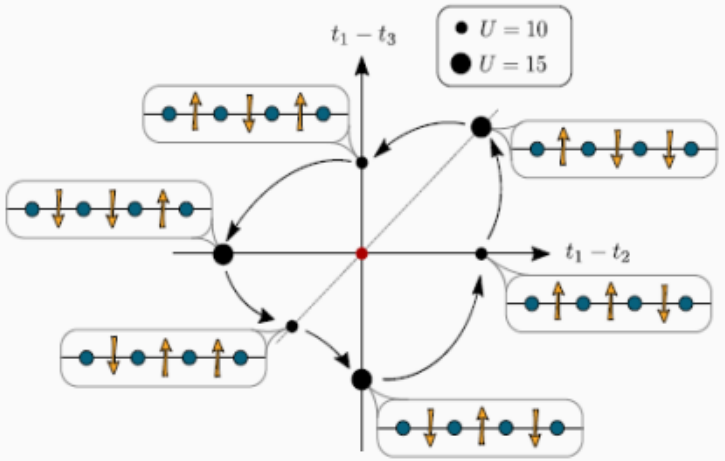


$$t_k = t + \alpha \langle \sigma_k^z \rangle$$

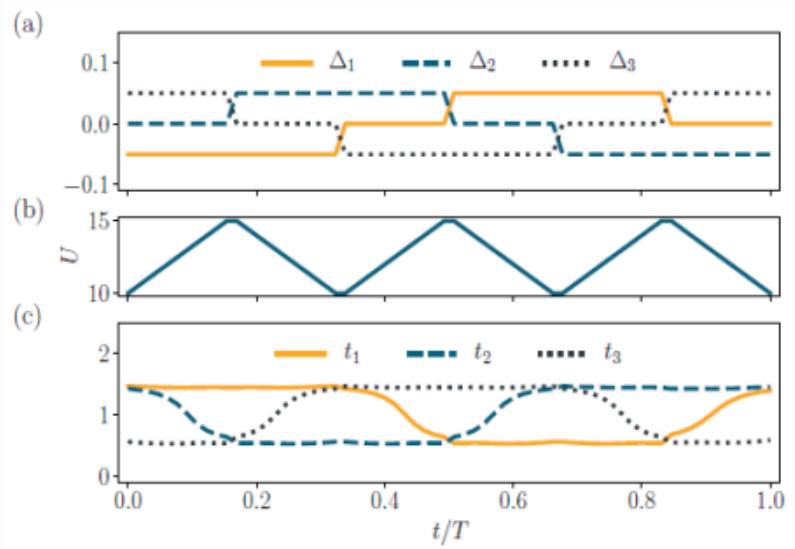


## Transported charge

$$P_L(t) = \frac{1}{L} \sum_j (j - j_0) \langle \Psi(t) | \hat{n}_j | \Psi(t) \rangle$$

$$\Delta P_L(t_i) = P_L(t_i^+) - P_L(t_i^-)$$

$$\Delta n_L = -\sum_i \Delta P_L(t_i)$$

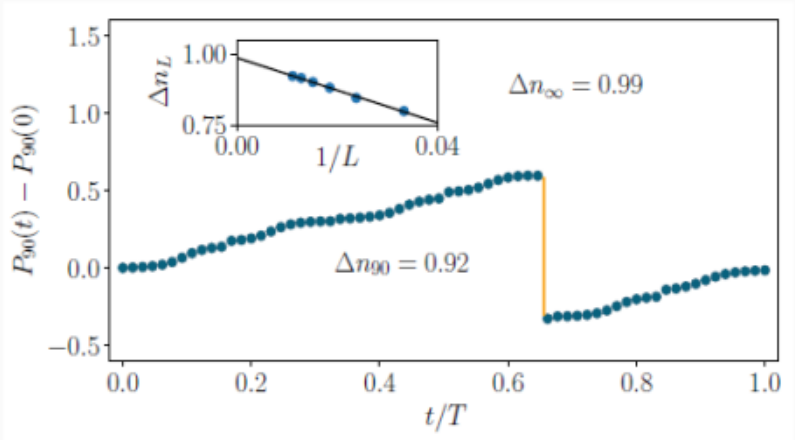

# Conclusions: Quantum Narcissism

Maciej Lewenstein was born in 1958 in Warsaw. He is a theoretical physicist and currently an ICREA professor at ICFO – Institut de Ciencies Fotniques in Castelldefels near Barcelona. He has written over 480 scientific papers and is the recipient of many international and national prizes. Next to theoretical physics his other passion is music and jazz in particular. His collection of records includes over 8000 entries.

*Maciej Lewenstein's book is a very important contribution to the history of jazz in Poland. This is a very detailed and profound volume that comes as a great aid to charting all of the most important Polish jazz recordings. I know of no other book of such kind. It is a definite must-read for both professionals and jazz enthusiasts – in Poland and beyond.*

Tomasz Stańko

*There is no other book already published on the subject, certainly nothing of such scope or including such detailed information. Although several books about Polish Jazz have been published in the last decade, none of them concentrate on Jazz recordings and they are mostly concerned with biographical and historical aspects of Polish Jazz. Therefore Mr. Lewenstein's book is in fact an ideal companion to those books already published.*

Adam Baruch

35 €
(VAT included)

ISBN 978-83-8022-012-6

Deloitte. fineVARE

ICFO *iCrea BOLT fortuna 1kg serpent.pl

POLISH JAZZ RECORDINGS & BEYOND

MACIEJ LEWENSTEIN

2.

POLISH JAZZ RECORDINGS & BEYOND

MACIEJ LEWENSTEIN

This book is a guide to Polish jazz recordings on CDs. It describes over 1900 discs in a systematic and organised way, with artists' names arranged alphabetically. It goes often beyond jazz and describes also discs with contemporary classical music or rock.